Theoretical Basis for Estimated Test Times and Conditions for Drop Tower and Space-Based Droplet Burning Experiments With Methanol and N-Heptane

MAE Report No. 1999

Anthony J. Marchese, Frederick L. Dryer
and Mun Y. Choi

August 1994

This work was supported by the NASA Lewis Research Center under the Grant no. NAG 3-1231 in preparation for the Science Requirements Documentation for the Droplet Combustion Experiment. Parts of this document appear within the Science Requirements Document as Appendix A.

Theoretical Basis for Estimated Test Times and Conditions for Drop Tower and Space-Based Droplet Burning Experiments With Methanol and N-Heptane

Anthony J. Marchese and Frederick L. Dryer
Department of Mechanical and Aerospace Engineering
Princeton University
Princeton, New Jersey 08544

Mun Y. Choi
Department of Mechanical Engineering
University of Illinois at Chicago
Chicago, IL 60607-7022

ABSTRACT

In order to develop an extensive envelope of test conditions for NASA's space-based Droplet Combustion Experiment (DCE) as well those droplet experiments which can be performed using a drop tower, the transient vaporization and combustion of methanol and n-heptane droplets were simulated using a fully time-dependent, spherically symmetric droplet combustion model recently developed at Princeton University. The transient vaporization of methanol and n-heptane was modeled to characterize the instantaneous gas phase composition surrounding the droplet prior to the introduction of an ignition source. The results for methanol/air showed that the entire gas phase surrounding a 2 mm methanol droplet deployed in zero-g quickly falls outside the lean flammability limit. The gas phase surrounding an identically-sized n-heptane droplet, on the other hand, remains flammable. The combustion of methanol was then modeled considering a detailed gas phase chemical kinetic mechanism (168 steps, 26 species) and the effect of the dissolution of flame-generated water into the liquid droplet. These results were used to determine the critical ignition diameter required to achieve quasi-steady droplet combustion in a given oxidizing environment. For droplet diameters greater than the critical ignition diameter, the model predicted a finite diameter at which the flame would extinguish. These extinction diameters were found to vary significantly with initial droplet diameter. This phenomenon appears to be unique to the transient heat transfer, mass transfer and chemical kinetics of the system and thus has not been reported elsewhere to date. The extinction diameter was also shown to vary significantly with the liquid phase Lewis number since the amount of water present in the droplet at extinction is largely governed by the rate at which water is transported into the droplet via mass diffusion. Finally, the numerical results for n-heptane combustion were obtained using both 2 step and 96 step semi-emperical chemical kinetic mechanisms. Neither mechanism exhibited the variation of extinction diameter with initial diameter.

INTRODUCTION

Isolated droplet combustion has been the subject of extensive experimental and theoretical investigations for more than 40 years. In the mid-1950's, theoretical developments [1, 2] led to the first general formulation for describing the burning characteristics of droplets, the so-called 'd^2-law'. This quasi-steady, one-dimensional model incorporated a number of limiting assumptions such as the thin flame-sheet approximation (infinite chemical kinetic rates), temperature-independent thermo-physical and transport properties, constant uniform droplet temperature, and unity Lewis number. The qualitative behavior of the 'd^2-law' formulation has been found to be essentially correct and, provided that appropriate selections for transport parameters are assumed, the burning rate of the

droplets can be predicted reasonably well. Experiments on spherically-symmetric droplet burning do, however, reveal qualitatively different behavior than 'd^2-law' predictions, indicating weaknesses in the assumptions of the analysis. Recent advances in asymptotic analyses with reduced chemistry [3-7] and time-dependent numerical approaches [8-18] have produced increasingly refined descriptions of temperature-dependent transport and chemical kinetic effects on burning rate, flame-standoff, flame temperature, droplet ignition, and droplet extinction, as well as other phenomena. Yet, much remains to be understood and advanced through additional experiments and further refinements in models, particularly concerning the transient nature and detailed structure of these phenomena.

Experimentally, drop towers have been successfully utilized to create microgravity environments wherein the effects of natural and forced convection can be minimized such that sphero-symmetric droplet combustion can be studied. These experiments are limited, however, to those sized droplets which can be grown, deployed, ignited, burned, and extinguished in the drop-time available. NASA Lewis Research Center, for example, has two drop towers which result in 2.2 seconds and 5.0 seconds of microgravity. In order to significantly extend the time available to study the combustion of an isolated liquid droplet, the space-based Droplet Combustion Experiment (DCE) is currently under development at NASA. In this experiment, single, isolated methanol and n-heptane droplets of up to 5 mm will be burned in nitrogen/oxygen and helium/oxygen environments at several ambient pressures and oxygen indices.

In order to develop an extensive envelope of test conditions for those experiments which can only be performed in space as well as those experiments which could be performed using the aforementioned drop towers, the combustion and vaporization of methanol and n-heptane droplets was simulated using a fully time-dependent, sphero-symmetric droplet combustion model recently developed at Princeton University. [8-18] The numerical model [8, 9], conceptually shown in Fig. 1, is generically formulated such that various levels of sub-model approximations for physical and chemical processes can be incorporated in both time and spatially dependent terms (See Fig. 2). These sub-models range from semi-empirical/ experimental correlations to extensive, temperature dependent databases for thermochemistry, complex chemical kinetics, and detailed molecular transport. The numerical model is capable of predicting time-dependent ignition, burning rate, flame standoff, and extinction phenomena, in addition to other parameters such as the critical ignition diameter (not previously addressed using either asymptotic or numerical methods) and the evolving chemical structure of the flame. To date, the numerical model has compared favorably with results from limited droplet combustion experiments conducted in the NASA-LeRC 2.2 second drop tower. The predictive capabilities of the model can, however, be substantially refined as more drop tower data become available for further validation studies.

In the following sections, the results of numerical modeling which was performed in conjunction with ground-based experiments in drop towers at NASA-LeRC and bench-scale experiments at Princeton University [14, 18] are presented. These results were successful in

generating extensive experimental test envelopes for future drop tower and space-based combustion experiments with methanol droplets in He/O_2 oxidizing environments and with n-heptane droplets in He/O_2 and N_2/O_2 environments. Of particular importance in developing these envelopes was the numerical computation of the following parameters:

- critical ignition diameter,
- total burn time, and
- extinction diameter.

These parameters will be described in detail below. For the methanol computations, a detailed gas-phase chemical kinetic mechanism which consisted of 26 species and 168 reactions was considered. In addition, the effect of water dissolution into the liquid droplet was considered in the methanol modeling. For the n-heptane studies, a 96 step semi-empirical gas-phase chemical kinetic mechanism was considered and compared with earlier results which utilized a semi-empirical, three-step mechanism.

TRANSIENT VAPORIZATION OF METHANOL AND N-HEPTANE DROPLETS [17]

Any ignition device utilized in a microgravity droplet combustion experiment has two primary requirements. Obviously, the first requirement of the device is that it must be capable of igniting the droplet. The second requirement is that the device must cause minimum disturbance of the droplet. This requirement suggests a device which achieves ignition with the lowest possible energy and deposits this energy symmetrically. While much work has been done in the past to understand the interactions between an ignition source (a spark, for instance) and a droplet [19], little was understood about the instantaneous evolution of the gas phase surrounding a droplet after deployment into the microgravity environment. Indeed, prior to this investigation, it was unclear whether it was possible to achieve pure gas phase ignition in the region surrounding a droplet, or if was always necessary to supply additional energy to the droplet surface to raise the droplet surface temperature thereby increasing the mass fraction of fuel in the gas phase.

Table 1. Combustion and Flammability Data for N-Heptane and Methanol

	N - Heptane	Methanol
Heat of Vaporization [cal/g]	76.5	262.5
Stoichiometric Fuel/O_2 Mass Fraction	0.284	0.667
Lean Flammability Limit [Vol%, Air, 1 Atm]	1.1%	6.7%
Flash Temperature [°C]	- 4	11.5

The fact that methanol and n-heptane have flash temperatures of 11.5 °C and -4 °C respectively would suggest the possibility of achieving pure gas phase ignition in the region surrounding such droplets deployed in air at 25 °C (See Table 1). However, experiments [10, 18] have shown that, under the same experimental conditions, methanol droplets are much more difficult to ignite than n-heptane droplets. In order to explain these experimental

observations and, if possible, determine the optimum location and energy content for a microgravity droplet ignition device, the numerical model described above was used to simulate the transient vaporization process of liquid methanol and n-heptane droplets after deployment into microgravity environments.

The modeling results have indicated that, although, methanol has a flash temperature of 11.5 °C, it would be extremely difficult to achieve pure gas phase ignition of a methanol droplet in the 1 mm size range deployed in air. As the definition of the flash temperature would suggest, initially a 25 °C droplet is surrounded by a thin layer of fuel/air mixture which is within the lean flammability limit of methanol/air. The results show that in short time periods after deployment the mere divergence of the flow field results in a finite gas phase location at which the gas mixture falls below its lean flammability limit. Due to the stoichiometry of the methanol/air system, this location is at most one radius from the droplet surface. Moreover, as the droplet vaporizes, the high latent heat of vaporization of methanol causes the surface temperature to rapidly drop. The gas phase location of the lean flammability limit thus moves closer to the droplet surface. After only several seconds, the droplet surface temperature falls below the flash temperature, at which time the entire gas phase surrounding the droplet is outside the lean flammability limit.

Figures 3a and 3b show the calculated droplet surface temperature and the gas phase location of the lean flammability limit for 25 °C droplets of methanol and n-heptane instantaneously immersed in atmospheric pressure air at 25 °C. These results suggest that only a precisely timed and located ignition source would be able to achieve pure gas phase ignition for the methanol/air system. An ignition source located outside the locus of flammable mixture would require an ignition energy much greater than the minimum gas phase ignition energy as additional energy would have to be diffusionally or radiatively supplied to raise the droplet surface temperature.

The results for n-heptane (see Figs. 3a and 3b) show precisely why it is less difficult to ignite n-heptane droplets than methanol droplets. Firstly, the stoichiometry of the n-heptane/air system results in a lean limit locus which is much further from the droplet surface than for the methanol/air system. Furthermore, while the vaporization of an n-heptane droplet does cause its surface temperature to drop, it does so at a much slower rate since its latent heat of vaporization (see Table 1) is roughly 1/4 that of methanol. These results suggest that, since the gas phase surrounding an n-heptane droplet remains flammable at distances of 3 radii from the droplet surface, pure gas phase ignition may be realizable for the n-heptane/air system.

Ignition of methanol droplets in 50% oxygen-helium mixtures at atmospheric pressure has been achieved in 2.2 second tower experiments using sparks. The discharge of a sparks aboard spacecraft is, however, undesirable since such electrical discharges result in substantial electromagnetic noise which can adversely affect spacecraft instrumentation. In addition, Shaw et.al [19] have shown that substantial relative motion of the gas phase relative to the droplet can be induced by sparks. It has thus been proposed that a hot wire ignition system be

developed for the DCE. To date, ground-based experiments suggested that methanol hot wire ignition was apparently constrained by the vaporization effects described above. Specifically, in order to ignite a methanol droplet it was necessary to place the hot wire very close to the droplet surface. Extrapolation of these observations to microgravity conditions is not possible and no drop tower data are presently available to demonstrate hot wire ignition of methanol droplets in helium-oxygen mixtures.

It should also be recognized that if the hot wire must be placed within 1 radius from the methanol droplet surface, it will be difficult to isolate the wire from the flame once a steady state flame develops since for methanol droplets the flame is located between 2 and 4 radii from the droplet surface. This situation is undesirable from several standpoints, such as limiting the hot wire lifetime, and contaminating the experiment via heat loss to the wires from the flame. Moreover, attempts to quickly retract the hot wire array will cause drag- induced convection in the vicinity of the droplet. While n-heptane droplets have been successfully ignited using the hot wire technique (in support of the above analysis), the steady-state flame standoff ratio of n-heptane is substantially greater than that of methanol. Thus, the issue of the proximity of the hot wire to the flame must still be addressed.

METHANOL DROPLET COMBUSTION

Methanol is a fuel for which considerable details for thermo-physical and thermo-chemical parameters are already known. The elementary detailed chemical kinetic mechanism for methanol oxidation is probably the most developed and tested of any liquid fuel oxidation mechanism and the species and reactions involved are relatively simplistic in comparison to those required for describing the oxidation of other hydrocarbons [20, 21]. The thermo-chemical and thermo-physical properties of the fuel, its combustion intermediates and products [22, 23], vapor-pressure characteristics [24], and the dissolution characteristics of combustion products/intermediates in methanol [25] are relatively well known. Furthermore, methanol burns without the complicating phenomena of soot formation [20, 21]. Details of the kinetic mechanism and elementary rate parameters are continuing to evolve [26-32] at a rapid pace. In the present work, a 168 reaction, 26 species kinetic model [9, 10, 26-28] was utilized in the numerical model. This chemical kinetic mechanism does not incorporate the pressure-dependent mechanistic effects studied more recently [29-32]. Model modifications to include such advances are in progress [18] and will be the subject of additional refinements for comparison with data obtained from future bench, drop tower, and space-based experiments.

Methanol droplet combustion exhibits particularly interesting characteristics because a number of the combustion products and intermediates, notably water and formaldehyde, are highly soluble in the fuel [10, 14, 33-36]. Various calculations have been performed and compared with the experimental data generated in the NASA-Lewis 2.2 second drop tower [10] and with ground-based droplet burning experiments [11, 14] which show evidence of product dissolution in the fuel droplet during combustion. Results of extensive numerical modeling of methanol combustion will be discussed below.

Droplet Ignition

The d^2 law of droplet combustion will predict the gasification rate of a liquid droplet with reasonable accuracy for instances in which the chemical reaction time is much shorter than the characteristic flow time of the system. Similarly, the d^2 law of droplet vaporization will predict the gasification rate of a liquid droplet accurately for the case of chemically frozen flow, i.e. for instances in which the characteristic time for chemical reaction is much longer than the characteristic flow time for the system. In realistic droplet combustion/vaporization situations, the preceding situations do not always exist. Figure 4 is a schematic representation of all possible steady state solutions of droplet combustion and vaporization plotted as a function of the system Dahmköhler number. This figure is the so-called droplet S-curve. [37] The Dahmköhler number is a ratio of the system flow time to the chemical reaction time where the characteristic flow time is merely the droplet radius squared divided by the mass diffusivity of the fuel. Therefore, the droplet S-curve suggests that, given a certain set of initial conditions, there will exist a minimum droplet diameter, below which the development of steady state droplet combustion is not possible. This diameter will be referred to as the critical ignition diameter. The critical ignition diameter corresponds to the lower turning point on the S-curve of Fig. 4 which occurs at the ignition Dahmköhler number, D_I.

While extensive theoretical studies have been performed to identify D_I using asymptotic techniques [37], such approaches cannot fully consider the effects of dynamics in crossing the limiting conditions. It is now possible to solve the fully-transient system numerically with detailed chemistry and molecular transport. The physical system represented by the numerical model is shown schematically in Fig. 5, while typical numerical results utilizing a sphero-symmetric ignition sub-model are shown in Fig. 6. A symmetric ignition process (Fig. 5a) was approximated by establishing a finite spherical shell of high temperature surrounding the methanol droplet [Fig. 6a]. Compared to likely experimental configurations, this "ignition source" is situated closer to the droplet surface and features a more disperse energy distribution than either sparks or hot-wires. The computed droplet heating and ignition times are considerably shorter than the experimentally observed value. (This has been taken into account in the experimental design). However, the predictions allow conservative estimates of critical ignition diameter to be obtained, and the ensuing combustion phenomena (Figs. 5b-5d, 6b-6d) to be studied.

Shortly after the introduction of the ignition source, the droplet begins to vaporize vigorously. Additional fuel vapor accumulates near the surface and diffuses outward, mixing with the ambient oxidizer. As the droplet continues to vaporize, the hot vapor-oxidizer mixture near the droplet surface begins to react (note the oxygen depletion near the drop surface in Fig. 6b), and a partially-premixed flame structure develops. Transition to a fully-developed diffusion flame surrounding the drop depends on the strength of the ignition energy,

the evolving heat release, and the dynamics of this transition, which are in turn influenced by the initial droplet diameter, oxygen index, diluent species, and ambient pressure.

Quasi-steady droplet combustion and vaporization as described by the d^2 law predicts a constant droplet gasification rate (time rate of change of d^2 with respect to time) whose value depends on the Dahmköhler number (see Fig. 4). The fully-transient numerical model used in the present investigation calculates an instantaneous gasification rate which continuously evolves during the ignition, steady combustion, and extinction conditions described in the preceding section. Figure 7 shows calculated instantaneous gasification rate vs. time for droplets with initial diameters ranging from 575 to 1500 microns deployed in a 35% O_2/ 65% He mixture at 0.5 atm and fixed ignition energy content. Referring to the 1500 micron case of Fig 7, the gasification rate initially increases well above the rate which characterizes sustained burning because of the localized energy of ignition and heat release from the partially-premixed reaction. The gasification rate then approaches a relatively constant value which roughly corresponds to that predicted by the d^2 law of droplet combustion. After a time period which constitutes the majority of the droplet burn time, the gasification rate suddenly drops as the flame extinguishes. As the residual enthalpy in the flame dissipates, the gasification rate approaches that predicted by the d^2 law of droplet vaporization.

Figure 7 shows that an initial droplet size is found below which transition to sustained burning does not occur, and the stimulated gasification rate subsides to the vaporization rate at ambient temperature. As initial diameter is further increased, conditions are found for which partial transition to diffusive sustained burning occurs. However, combustion prematurely ceases. Finally, as the initial drop diameter is further increased, sustained burning is achieved, and the combustion continues until droplet burning extinction conditions are reached. The underlying physical phenomena governing the transition from non-burning to sustained burning states will be discussed in the following section. Figure 8 shows that similar ignition transitions are predicted when the initial droplet diameter is held constant and the oxygen index is varied. For a given initial diameter, an oxygen index can be found below which any realistic amount of ignition energy fails to establish sustained burning. As oxygen index is increased, partial transition to sustained burning occurs. With further increases, sustained burning is finally achieved.

By performing extensive similar numerical experiments, critical ignition diameter criteria as a function of oxygen index, inert diluent, and ambient pressure were determined (Figure 9). The test envelope for droplet combustion experiments is defined such that sustained burning should be achieved for a majority of the test points within the envelope and the initial drop diameter is from two to three times the critical ignition diameter.

Droplet Extinction

As sustained droplet burning continues [see Figs. 5c, 6c], the droplet size continuously regresses resulting in a decreasing Dahmköhler number. Eventually, a droplet diameter is

reached for which the characteristic system flow time [r^2/D] becomes the same order as the characteristic chemical time. As this occurs, substantial leakage of both fuel and oxidizer through the reaction zone occurs [See Figure 6d], the gas-phase radical pool precipitously decays, the flame temperature drops, the burning rate is dramatically reduced, and the droplet becomes extinguished. This state corresponds to the extinction Dahmköhler number, D_E [see Fig 4]. The droplet diameter at this state is referred to as the extinction diameter. Figures 7 and 8 clearly show that the numerical model predicts an abrupt change in gasification rate which occurs at a finite diameter. Accordingly, the model was used to numerically determine an extinction condition as a function of initial droplet size, inert diluent, oxygen index, and ambient pressure.

From an experimental point of view, it is desirable to choose operating conditions which result in extinction droplet diameters of 200 microns or greater. At extinction diameters less than 200 microns, the dynamics of flame extinguishment are difficult to experimentally observe, and the numerical calculations show that, although gas phase chemistry has been "extinguished", vigorous droplet gasification may continue due to residual enthalpy in the extinguished gas phase surrounding the droplet. At extinction diameters larger than about 200 microns, the residual enthalpy results in minimal reductions in the drop diameter from that at extinction, and the experimentally observed droplet diameter is an accurate parameter for indicating the extinction condition.

Larger, more well-defined extinction diameters can be achieved experimentally for droplet combustion in general, and for methanol and n-heptane specifically, by utilizing helium rather than nitrogen as the inert [10, 14]. The combination of higher thermal conductivity (to increase the droplet burning rate) and higher thermal diffusivity for helium (to increase the reactant leakage and thus decrease the flame temperature) result in much larger extinction diameters than for similar conditions with nitrogen as diluent. In the experimental results shown in Figures 10a-b, methanol droplets burning in oxygen-helium environments displayed higher burning rates than for corresponding oxygen-nitrogen systems. After the droplet surface regressed to a diameter of 400 microns, the flame extinguished, causing a drastic reduction in the burning rate. The average extinction diameter for this condition was found to be 350 microns which was in good agreement with the computational results (Table 2).

Table 2. Methanol Parameter Comparisons for 1.5mm inital droplet diameter in 50%He/50% O_2 at 1 atm. pressure. [From Ref. 10]

	Experiment	Model	'd^2-law'
Burning Rate [mm^2/s]	1.3	1.4	1.8
Flame Standoff Ratio	3.5	3.1	5.4
Extinction Diameter [micron]	350	300	Cannot Predict

These methanol droplet experiments (Figs. 10a-b), as well as others conducted with nitrogen as diluent, display non-'d^2-law' gasification behavior due to diffusive transport to and subsequent condensation of flame-generated products and intermediates on the fuel droplet

surface [10, 14, 31]. These phenomena modify the burning rate of the droplet, similar to what was proposed earlier for alcohol vaporization in moist environments [36]. Ground-based pool-burning experiments [34] in air (atmospheric pressure) and freely-falling droplet combustion experiments on small droplets in both ambient temperature oxygen [14, 16, 35] and in hot post-combustion gases from oxygen-rich flames in nitrogen [37] (atmospheric pressure) show that substantial water absorption and dissolution occurs at the droplet surface. The pure oxygen, cold environment experiments also show that formaldehyde is absorbed by and dissolved into the liquid phase. Figure 11 shows the results of freely-falling droplet experiments wherein methanol droplets were collected, quenched, and analyzed [14]. In these experiments, the time history of the droplet water and formaldehyde content was determined by placing a cooled probe at different vertical locations in the droplet trajectory. Also, suspended droplet experiments were performed wherein methanol/water mixture droplets were burned to extinction at which time they were sampled to determine the water content at extinction [14]. The results showed that when the initial water content varied from 20-50% the measured water content at extinction remained relatively constant (78-86%). These results are summarized in Table 3.

Table 3. Suspend Methanol/Water Droplet Results [From Ref. 14]

Initial H_2O Concentration	Final H_2O Concentration
20.0 %	78 ± 2 %
30.1 %	81 ± 2%
40.2 %	81 ± 2 %
49.8 %	84 ± 2 %
49.8 %	86 ± 2 %

In order to investigate the experimentally-observed effect of the dissolution of flame-generated products on the combustion of methanol droplets, the numerical model described above was formulated to include the dissolution of water into the methanol droplet [10, 14, 18, 38]. Since the total amount of formaldehyde observed was negligible compared to the water, the dissolution of formaldehyde was not considered in this first study. Numerical calculations show that water absorption and dissolution first increases the surface concentration of water, resulting in increased droplet surface temperatures. Eventually, water is re-vaporized at the droplet surface as well as diffused into the droplet interior. Numerical results clearly show that this re-vaporization of water results in a decrease in heat release and thus a decrease in flame temperature [10, 14, 18, 38]. This decrease in flame temperature decreases the Dahmköhler number and, thus, promotes extinction. Recent asymptotic calculations also support this conclusion [7]. It should be noted here that both pool burning in air and free-falling droplet experiments in ambient temperature, pure oxygen with n-heptane as fuel display negligible product and intermediate absorption during the combustion period [14, 35].

The total amount of water absorbed by a methanol droplet ultimately depends on the mass transport of water into the methanol droplet. Since the model described in this investigation is sphere-symmetric, one-dimensional, and the temperature variation within the

droplet was found to be small, a single parameter was sufficient to specify the mass diffusivity of water in methanol. Accordingly, a liquid phase Lewis number was defined as follows:

$$Le_l = \frac{\text{Thermal Diffusivity of } CH_3OH \text{ Droplet}}{\text{Mass Diffusivity of } H_2O \text{ into } CH_3OH} = \frac{(\lambda/\rho C_p)_l}{\mathcal{D}_{H_2O,l}}$$

Figure 12 shows the instantaneous total integrated amount of water present in the liquid phase after ignition for various values of the liquid Lewis number. A droplet with a liquid Lewis number much greater than unity will undergo very little water dissolution over its lifetime. In this case, assuming equilibrium conditions at the gas-liquid interface, a thin boundary layer of water will develop in the liquid droplet near the surface as diffusion of water inward is slow. Conversely, a low liquid Lewis number promotes water dissolution as water absorbed at the surface readily diffuses inward.

Figure 13 is a plot of calculated extinction diameter as a function of liquid Lewis number. As the above arguments would suggest, decreasing the liquid Lewis number results in an increase in the total amount of water dissolved which, when re-vaporized, decreases the flame temperature which, in turn, promotes extinction [18, 38]. In terms of known properties, the Lewis number for the liquid methanol/water system is about 45 at room temperature [39]. As Fig 12 would suggest, the high Lewis number of the methanol/water system should result in little overall water dissolution over the droplet lifetime. However, the "effective" Lewis number may be considerably smaller if internal liquid phase circulations are present. Such circulations can be induced by gas phase convection relative to the droplet during combustion, and by the experimental initial droplet growth and deployment techniques which are utilized. Figure 13 shows that as the "effective" Lewis number approaches that defined by the liquid properties themselves, the derived extinction diameter becomes independent of Lewis number.

The numerical results of Fig. 12 could, in theory, be used to determine the "effective" liquid Lewis number that was present in the experiments which were used to generate the data in Fig. 11. There are, however, major differences between the sphere symmetric numerical model and any data obtained in a freely-falling droplet apparatus. Not only are internal circulations present due to the forced convection on the droplet, but, the rate at which flame produced water arrives at the droplet surface may differ significantly from the sphere symmetric case. Similar arguments can be applied to the suspended droplet results presented in Table 3 wherein free-convection was present. In space-based or drop tower based microgravity experiments, internal circulation may also be present in the droplet as a result of the deployment technique. However, since free and forced convection are minimal, the one-dimensional, spherical flame will result in purely diffusional transport of water to the droplet surface. Therefore, the numerical model will still be valid if an appropriate "effective" Lewis number can be determined which takes into account the enhanced internal mass transfer due to internal droplet circulation.

Figure 14 compares asymptotic and numerical predictions of extinction diameter for ambient temperature, helium-oxygen conditions at one atmosphere pressure. The asymptotic results (dotted lines) are shown for two different assumed concentrations of absorbed water at the droplet surface. The numerical results (unconnected data points) were calculated for different initial diameters (numbers adjacent to data points, in microns) and two different oxygen indices (25% and 35%). The numerical results, thus, predict that for a given pressure, oxygen index, and liquid-phase Lewis number, the extinction diameter is not a constant, but rather, varies with the initial diameter. The results show that for initial diameters less than approximately 3 times the critical ignition diameter, the droplets extinguish prematurely. In fact, the extinction diameter decreases with increasing initial diameter until the initial diameter is increased to approximately 3 times the critical ignition diameter. At initial diameters greater than approximately 3 times the critical ignition diameter, the extinction diameter is predicted to increase, but only slightly. This is shown graphically in Fig. 15 where extinction diameter is plotted vs. initial diameter.

These results appear to be predominantly due a continuous evolution of the flame structure, as well as the effect of water absorption/dissolution at the droplet surface. No similar behavior has been described in the literature previously. No experimental data are available to either support or refute these predictions. Figs. 7 and 8 show that for each condition, the macroscopic property of droplet gasification rate reaches a value which is nearly constant for an extended period of time in agreement with experiment. However, the numerical modeling results also show that even while a macroscopic property such as the gasification rate may appear to be quasi-steady, the underlying processes of chemistry and transport may be continuosly evolving. Earlier finite chemistry studies predict that with decreasing Dahmköhler number, the rate of leakage through the flame zone increases resulting in a decrease in flame temperature. The present numerical study suggests that not only does the flame temperature vary with droplet diameter, but the entire flame structure contiuously evolves throughout the droplet lifetime. Figure 16 shows the continuous time evolution of the gas phase heat release profile for the 575, 675, and 1500 micron initial diameter cases of Fig. 7. The figure shows that for the 575 and 675 micron droplets the heat release is exothermic everywhere in the gas phase for the entire droplet lifetime. For the 1500 micron droplet, there exists significant endothermicity between the droplet and the flame for the first full second of the droplet lifetime. During the latter stages of the droplet lifetime, the heat release profile becomes exothermic everywhere in the gas phase, and in fact, appears similar to that of the smaller droplets which extinguished prematurely. In summary, these results have shown that for methanol, the well validated, yet conceptually simple chemical kinetic oxidation mechanism coupled with the fully-transient numerical model has resulted in the prediction of an entire regime of droplets which ignite, but extinguish early. As will be discussed below, the semi-empirical mechanism of Warnatz which was used for n-heptane calculations did not exhibit this phenomenon.

The minimum extinction diameter determined from numerical calculations for a particular ambient pressure and oxygen index was utilized to determine the experimental test envelope for future drop tower and space-based experiments (see discussions below).

NORMAL ALKANE DROPLET COMBUSTION

Normal-heptane and n-decane have been utilized in many prior droplet burning studies, both in earth's gravitational field [e.g. 40] and in drop towers [e.g. 13, 41-44]. Under microgravity droplet combustion conditions, both exhibit significant soot formation and accumulation (by thermophoresis) within the surrounding diffusion flame [13, 42, 45]. The "sootshell" thus formed and the soot agglomerate densities within it are strongly influenced by ambient pressure, oxygen indices, and diluent species [11, 14], as well as by initial droplet size [45] and relative gas/droplet convection [43]. Associated with the formation and presence of the sootshell, is a reduced droplet gasification rate that can be as much as 40% lower than observed in early drop tower measurements at similar drop sizes (no sootshells present). The burning rate data increase with increasing relative gas/droplet convection rate [14, 43], and recent experiments [11] show that, contrary to classical theory, the gasification rate is increased significantly by pressure reduction (through reduced sooting). No fundamental theory has been conclusively established for these effects, but it has been suggested that radiation losses from the sootshell, changes in the temperature-averaged transport properties, and changes in gas-phase volume flux due to soot formation are possible sources of effects which change both the surface gasification rate and flame position [11, 14, 15].

Over some ranges of experimental parameters, droplet disruption and dismemberment is also observed to occur early in the droplet burning history [14, 42, 43], while over other ranges of conditions, droplet extinction is observed to occur. Speculations for the mechanisms which produce disruption are:

- deposition of high-molecular-weight soot precursor intermediates in the liquid phase, resulting in multi-component droplet gasification behavior [42, 46],
- collapse of the diffusion flame structure into the soot shell, causing intense disturbances from the soot shell ignition,
- soot deposition at the liquid surface, and,
- critical electrostatic charge accumulation in the soot shell and/or droplet surface [47].

Recent experiments at one-g suggest that deposition of high molecular weight components is insignificant [14, 34], and a clear explanation of the disruption phenomena remains to be established.

Unfortunately, thermo-physical, thermo-chemical, and chemical kinetic properties for these alkanes are not very well defined [8, 12]. For example, experimental values of thermo-physical parameters for n-heptane have been determined only at low temperatures. While theoretical evaluations based on ideal gas properties exist, calculated and experimental parameters are in significant disagreement. (See Table 4). In the present work, experimental values were utilized where available [48] and supplemented with theoretical estimations

assuming ideal gas properties. Transport and thermochemical data were estimated by using TRANSPORT PACKAGE and CHEMKIN codes [22, 23].

Table 4. Heat capacity for n-heptane vapor [kJ/kgK].

T [K]	Experimental	Theory
300	2.263	1.665
400	2.720	2.107
500	3.410	2.510
1000	Unavailable	3.811
1500	Unavailable	4.445

More importantly, the detailed kinetic mechanisms for large alkanes are only qualitatively understood [20, 21]. A 96 step semi-empirical mechanism has been proposed by Warnatz for predicting laminar pre-mixed flame propagation [49] for n-heptane-air flames, and this work has formed the basis for several studies on diffusion flames and reduced' model development [50, 3-5]. The principal empiricism in the Warnatz model is the description of n-heptyl radical decomposition into the unlikely products of $CH_3 + 2\ C_3H_6$ (in fixed ratio) rather than the expected mixture of β-scission products, C_2H_4, C_2H_5, C_3H_6, C_4H_8, CH_3, and C_5H_{10} [20], which are, in fact, evidenced in n-heptane-air diffusion flame structures [51] and flow reactors [52]. More complex detailed kinetic mechanisms have been developed for autoignition studies in engines (up to 5000 reaction steps), but these mechanisms involve considerable uncertainty and low and intermediate oxidation chemistry of little relevance in diffusion flames. In the present study, a 2 step semi-empirical mechanism was used along with as the 96 step Warnatz mechanism described above.

Rate ratio asymptotic methods have also been utilized extensively to predict flame structure and extinction diameter for n-heptane droplet combustion in nitrogen [3-6]. An assumed, minimal set of detailed reactions for the oxidation of n-heptane was used to produce a two, three, or four step reduced mechanism by the systematic application of partial-equilibrium and steady-state assumptions. Using the derived mechanisms, the structure of spherically symmetric diffusion flames around an n-heptane droplet have been analyzed using rate-ratio asymptotics. The outer transport zones were described by the classical flame-sheet analysis. The inner structure consisted of a thin fuel-consumption layer on the rich side of the flame where fuel and H radical consumption occur and some CO and water are produced, and a broader but still thin oxidation layer on the lean side where the remaining H_2 and CO are oxidized. In addition to varying the complexities as to how the outer oxidation zone is structured, the work has considered two options as to how n-heptyl radicals are converted to CO and H_2:

a) n-heptyl radicals pyrolyze to propene and methyl radicals with subsequent reactions of these species forming CO and H_2;
b) n-heptyl radicals pyrolyze to ethene and methyl radicals with subsequent reactions of these species to CO and H_2.

In each case, the theory identifies a scalar dissipation rate, related to the droplet diameter appropriate for droplet burning. From the analysis, the variations in flame temperature and in species concentrations with the stoichiometric scalar dissipation rate X_{st} were obtained. Since extinction occurs where X_{st} reaches a maximum, the extinction diameters for n-heptane droplets were estimated from the results for different pressures and ambient oxygen concentrations. Figure 17 shows the results of the most recent work [5] in which a four step reduced kinetic analysis was performed and compared with those for earlier two- and three-step approximations, and the assumption of propene formation. While the two step mechanism is suggested to yield the most realistic predictions of extinction diameter, it also is noted to produce oversimplified flame structure. It is observed that these analyses and those performed numerically all show the same qualitative function behavior of extinction diameter with oxygen indices and pressure. However, quantitatively, the various theoretical approaches produce values of d_{ext} for the same conditions that vary by approximately a factor of two or more. Similar discrepancies are found when nitrogen diluent is replaced by helium. These quantitative differences are likely to only be further resolved by improved definition of an appropriate kinetic model for n-heptane kinetics for droplet combustion and validating experimental measurements of the extinction diameter.

Table 5. Semi-empirical kinetic data for n-heptane.

$C_7H_{16} + 7.5O_2 \rightarrow 7CO + 8H_2O$
$k_{ob} = 2x10^{14}[nC_7H_{16}][O_2]\exp(-40/RT)$
$CO + 0.5O_2 \leftrightarrow CO_2$
$k_{ob,f} = 10^{14.6}[CO][H_2O]^{0.5}[O_2]^{0.25}\exp(-40/RT)$
$k_{ob,b} = 5x10^{8}[CO_2]^{0.25}\exp(-40/RT)$

As a first approach to numerically predicting n-heptane droplet combustion parameters, computations were performed using 2 step semi-empirical kinetics with reversible CO/CO_2 chemistry (See Table 5). Numerical constants in the kinetic mechanism were adjusted to reproduce suspended droplet extinction diameter data [53] of n-heptane at low pressure (no soot formation). These results are summarized in Table 6.

Calculations similar to those described in the previous section for methanol were then performed to determine the burning characteristics of isolated n-heptane droplets under various ambient pressures, oxygen indices, and diluent. Critical ignition diameters were determined for helium and nitrogen diluents by varying the ignition energy (the location of the ignition temperature distribution relative to the droplet surface, the maximum temperature, and the energy content of the thermal wave), and initial droplet diameter.

Table 6. Extinction diameter for n-heptane droplets.

Yo	Pressure	Experimental	Calculated
.232	125 torr	0.34 mm	0.34 mm
.232	100 torr	0.42 mm	0.46 mm
.230	275 torr	0.59 mm	0.65 mm
.253	175 torr	0.29 mm	0.35 mm
.253	150 torr	0.37 mm	0.45 mm

As in the case of methanol droplets at the critical ignition diameter, the combination of the thermal energy transport to the ambient environment and that absorbed by the vaporization processes deplete the ignition energy from the flammable regions at a rate more rapid than the critical chemical heat release rates required for ignition. As oxygen index is decreased, the amount of energy required to achieve ignition increases, and at a limiting oxygen index, no ignition energy can be found which will initiate droplet combustion. As expected, the critical ignition diameter was considerably increased by substitution of helium for nitrogen diluent and by reducing the pressure (Fig. 18). However, extinction conditions were also shifted to higher oxygen indices by diluent substitution. Numerical calculations were also performed for n-heptane droplets to determine extinction diameter as a function of ambient conditions and inert diluent. Calculated extinction diameters are shown in Fig. 19.

No significant variation of extinction diameter with initial diameter was observed using the 2 step semi-empirical kinetic mechanism. Indeed, the transition phenomena from transient to sustained burning which was observed for methanol was not observed for these n-heptane calculations. This is not surprising, given the lack of detailed kinetics and the high activation energy for the overall conversion of n-heptane to carbon monoxide and water.

Next, the numerical model was modified to include the full semi-empirical, 96-step n-heptane oxidation mechanism of Warnatz [49]. This chemical mechanism effectively calculated quasi-steady gasification rate, temperature and species profiles and predicted finite extinction diameters. However, the additional detail provided by this mechanism was still not sufficient to predict the transition phenomena which was observed for methanol. A closer examination of the mechanism reveals that the only route for breakdown of the C_7H_{16} is via attack by radicals O, OH, and H. Moreover, since initially there exists only fuel, oxidizer, and inert in the gas phase, the only initial source of radicals in this mechanism is via oxygen dissociation. Indeed, ignition was not obtained for any initial conditions when the $O_2+M \rightarrow O+O+M$ reaction was surpressed. In short, while this mechanism may be adequate for steady state analyses in which a radical pool already exists, it does contain sufficient detail to capture the detailed ignition phenomena.

EXPERIMENTAL TEST ENVELOPE FOR GROUND AND SPACE-BASED EXPERIMENTS

In this section, the insights gained from the experimental, computational and asymptotic studies are combined to define test matrix envelopes for future ground-based and space-based experiments on n-heptane in helium-oxygen, n-heptane in nitrogen-oxygen, and methanol in helium-oxygen droplet combustion. The order in which these envelopes are presented reflects the current status of engineering developments on testing n-heptane and methanol experimental systems for 5.0 second drop tower and space-based experiments.

It is important to conduct all experiments under conditions of reduced sooting. While methanol droplets never soot, there are three methods which can be used to reduce sooting during n-heptane microgravity droplet combustion. The first method is to use reduced oxygen concentrations, which lowers the flame temperature and therefore the rate of fuel pyrolysis. Pressure reduction has also been found to curtail the production of soot [54]. Finally, the replacement of nitrogen with helium as the inert further reduces the sooting propensity of the droplets [11, 14]. Ground-based suspended droplet studies were utilized to determine the interactions of ambient pressure, diluent substitution, and oxygen index which suppress sooting for n-heptane droplet combustion [11, 14]. The limiting sooting condition was defined as that which resulted in burning rates near those for the non-sooting conditions. Comparison of suspended droplet results with 2.2 second tower experiments were performed to validate the extrapolation of ground-based data to microgravity conditions.

The critical ignition and extinction diameters, as numerically calculated above, in large measure determine the appropriate envelope of conditions over which microgravity droplet burning experiments can be conducted. The range in oxygen concentrations that can be studied is determined by ignition [lower limit] and sooting [upper limit] limitations. The lower limit for the initial droplet size that can be used is bounded by the restrictions on the critical ignition diameter and by the minimum diameter required for production of low residual velocities induced by droplet deployment. The smallest initial diameter which can be studied utilizing the droplet generation and deployment mechanisms currently proposed for DCE is 1mm. For droplets smaller than this diameter, the deployment mechanism has been found to impart unacceptable residual motion to the free droplet. Residual droplet motion scales approximately with the droplet mass. Finally, measured extinction diameters less than approximately 0.2 mm will be difficult to characterize due to the rapidity with which continued gasification will occur from residual gas enthalpy at extinction. Figures 20-28 display the composite regions where successful experiments for each of the noted fuel/diluent/ambient pressure conditions could be performed.

From the studies in the 5.0 second drop tower, the particular ranges of initial conditions shown in these figures can be related to test-time requirements. A unique feature of the DCE project is that the experimental methodology produces the highest degree of spherically symmetric conditions (spherical droplet with low relative drop/gas velocity). The

required time for each of the necessary engineering procedures (estimated from 5.0 second drop tower experiments using n-heptane droplets) is listed in Table 7.

Insufficient drop tower studies have been performed to identify these same parameters for methanol droplets. The parameters for growth and deployment of methanol droplets are therefore based on the above data. Using these data along with the calculated burning rates and extinction diameters, the required observation times for test conditions within any of the above test envelopes were estimated. Figure 29 presents a typical result of such calculations which were also used to define the appropriate test venue. It should be noted here that the limiting diameter of 1.56 mm for 5.0 second drop tower tests on n-heptane droplets in helium at one atmosphere pressure, coupled with the 1 mm lower bound for droplet initial size represents an insufficient range for parametric investigations for evaluating spherically symmetric droplet combustion characteristics. It is important that a droplet combustion experiment display a quasi-steady burning regime prior to the occurrence of extinction. Furthermore, extinction at large diameters (> 200 microns) is desired because it assures that continued vaporization (from the residual enthalpy in the droplet and the surrounding gas) will have a negligible effect.

Table 7. Engineering function times. [From Ref. 14]

Droplet Diameter [mm]	Growth Time	Stretch Time	Deploy &Ignition [Seconds]	Total Time
1.0 0	0.32	0.73	0.32	1.37
1.50	0.62	0.79	0.32	1.73
1.75	0.83	0.82	0.32	1.97
2.00	1.12	0.85	0.32	2.29
2.50	2.12	0.94	0.32	3.28
3.00	3.33	1.03	0.32	4.68
4.00	7.59	1.20	0.32	9.11

Finally, a series of numerical experiments were conducted to determine the effect of the uncertainty in operating conditions on the observable experimental data. Table 8 is a summary of the results of these calculations which were performed by perturbing the oxygen content, ambient pressure, and relative humidity of a baseline condition consisting of a 1.5 mm methanol droplet deployed in a 30% O_2/70% He oxidizing environment at 1 Atm. The results indicated that, at this condition, a ± 1% uncertainty in oxygen content corresponds to an uncertainties of 60 K, 0.04 mm^2/s, and 60 micron, respectively, in flame temperature, gasification rate, and extinction diameter. These results suggest that the oxygen index be known to within at most ± 0.5% uncertainty.

Table 8. Operating condition uncertainty calculations. Baseline condition: CH_3OH/30% O_2/ 70% He, 1 Atm, d_0 = 1500 micron.

at t = 1.0 s

Oxygen Index [%]	Gasification Rate [mm^2/s]	Flame Temperature [K]	Flame Standoff [d_f/d_L]	Extinction Diameter [micron]
29.0	1.068	1551	3.64	296
29.5	1.078	1564	3.60	278
30.0	1.090	1581	3.49	269
30.5	1.097	1597	3.50	252
31.0	1.105	1610	3.50	240

Relative Humidity [%]	Gasification Rate [mm^2/s]	Flame Temperature [K]	Flame Standoff [d_f/d_L]	Extinction Diameter [micron]
0.0	1.090	1581	3.49	269
10.0	1.088	1584	3.49	270

Ambient Pressure [Atm]	Gasification Rate [mm^2/s]	Flame Temperature [K]	Flame Standoff [d_f/d_L]	Extinction Diameter [micron]
0.95	1.088	1572	3.49	277
1.00	1.090	1581	3.49	269
1.05	1.090	1589	3.51	251

SUMMARY AND CONCLUSIONS

The transient vaporization and combustion of methanol and n-heptane droplets were simulated using a fully time-dependent, spherically symmetric droplet combustion model which was recently developed at Princeton University. The results of this study were successfully utilized to generate an extensive envelope of test conditions for NASA's space-based Droplet Combustion Experiment. Moreover, the extensive numerical computations required for this study have yielded interesting and previously unreported droplet combustion phenomena. Namely, the conceptually simple yet substantially validated gas phase chemical kinetics of methanol have provided sufficient detail to observe a continuously evolving flame structure as well as family of burning droplets which ignite but prematurely extinguish. Conversely, the semi-empirical n-heptane chemical kinetic mechanisms used in this study produced no such results. Further drop tower and space-based testing will be performed in the near future which, along with continuing numerical and analytical efforts will further our understanding of these phenomena.

ACKNOWLEDGEMENTS

This work has been supported by NASA Lewis Research Center under Grant No. NAG 3-1231. The authors gratefully acknowledge the helpful discussions with Dr. M. Vedha-Nayagam and Mr. John B. Haggard, Jr. at NASA LeRC and Professor Forman A. Williams at University of California, San Diego.

REFERENCES

1. Godsave, G. A. E., 1953, Studies of the Combustion of Drops in a Fuel Spray - The Burning of Single Drops of Fuel, Fourth Symposium (International) on Combustion, Williams and Wilkins Co., Baltimore, pp. 818-830.

2. Spalding, D. B., 1953, The Combustion of Liquid Fuels, Fourth Symposium International) on Combustion, Williams and Wilkins Co., Baltimore, pp. 847-865.

3. Card, J. M. and Williams, F. A., 1992, Asymptotic Analysis of the Structure and Extinction of Spherically Symmetrical n-Heptane Diffusion Flames, Combustion Science and Technology 84, pp. 91-119.

4. Card, J. M. and Williams, F. A., 1992, Asymptotic Analysis with Reduced Chemistry for the Burning of n-Heptane Droplets, Combustion and Flame 91, pp. 187-199.

5. Card, J. M., 1993, Asymptotic Analysis for the Burning of n-Heptane Droplets Using a Four-Step Reduced Mechanism, Combustion and Flame, 93, 375.

6. Williams, F. A., 1993, Studies of Droplet Burning and Extinction, Second International Microgravity Combustion Workshop, NASA Conference Publication 10113, pp. 283-290.

7. Zhang, B. L., Card, J. M., and Williams, F. A., 1994, Application of Rate Ratio Asymptotics to the Prediction of Extinction for Methanol Droplet Combustion. Submitted to the Twenty-Fifth International Symposium on Combustion, Irvine, CA.

8. Cho, S. Y., Yetter, R. A. and Dryer, F. L., 1990, Mathematical Modelling of Liquid Droplet Combustion in Micro gravity, Proceedings of the Seventh International Conference on Mathematical and Computer Modelling, Math. Comp. Modelling, 14, p. 790.

9. Cho, S. Y., Yetter, R. A. and Dryer, F. L., 1992, A Computer Model for One-Dimensional Mass and Energy Transport in and around Chemically Reacting Particles, Including Complex Gas-Phase Chemistry, Multicomponent Molecular Diffusion, Surface Evaporation and Heterogeneous Reaction, Journal of Computational Physics, 102, pp. 160-179.

10. Cho, S. Y., Choi, M. Y., and Dryer, F. L., 1991, The Extinction of A Methanol Droplet in Microgravity, Twenty Third Symposium (International) on Combustion, The Combustion Institute, p. 1611.

11. Choi, M. Y., Cho, S. Y., Dryer, F. L., and Haggard, J. B., Jr., 1991, Some Further Observations on Droplet Combustion Characteristics: NASA LeRC-Princeton Results, IKI/AIAA Microgravity Science Symposium, Moscow, May 12-21, 1991. Published as an AIAA Proceedings, H.C. Gatos and L.L. Regal, Chairs, (ISBN 1-56347-001-2). p. 294.

12. Choi, M. Y., Cho, S. Y., Dryer, F. L. and Haggard, J. B., Jr., 1992, Computational/Experimental Basis for Conducting Alkane Droplet Combustion Experiments on Space Platforms, Microgravity Fluid Mechanics, H.J. Rath, ed., Springer-Verlag, Berlin, pp. 337.

13. Choi, M. Y., Dryer, F. A., Card, J. M., Williams, F. A., Haggard, J. B., Jr. and Borowski, B.A., 1992, Microgravity Combustion of Isolated n-Decane and n-Heptane Droplets, AIAA Paper No. 92-0242, January.

14. Choi, M. Y., 1992, Droplet Combustion Characteristics under Micrograavity and Normal Gravity Conditions, Ph.D. Thesis, Mechanical and Aerospace Engineering Department, Princeton University, August. MAE Report No. T-1937

15. Choi, M. Y., Dryer, F. L., Green, G. J. and Sangiovanni, J. J., 1993, Soot Agglomeration in Isolated, Free Droplet Combustion, AIAA Paper No. 93-0823, January.

16. Dryer, F. L., 1993, Computation/Experimental Studies of Isolated, Single Component Droplet Combustion, Second International Microgravity Combustion Workshop, NASA Conference Publication 10113, pp. 291-296.

17. Marchese, A. J., and Dryer, F. L., 1993, Computational Modeling of Transient Methanol Droplet Vaporization, Eastern Sectional Meeting of the Combustion Institute, Princeton University, Princeton, NJ, October 25, 27.

18. Marchese, A. J., and Dryer, F. L., 1994, Work in progress.

19. Shaw, B. D., Dryer, F. L., Williams, F. A., and Gat, N., 1988, Interaction Between Gaseous Electrical Discharges and Single Liquid Droplets, Combustion and Flame 74, pp.233-254.

20. Westbrook, C. K. and Dryer, F. L., 1984, Chemical Kinetic Modeling of Hydrocarbon Combustion, Prog. Ener. Comb. Sci., 10, 1.

21. Dryer, F. L., 1991, The Phenomenology of Modeling Combustion Chemistry," Chapter 3 from Fossil Fuel Combustion: A Source Book, W. Bartok and A.F. Sarofim editors, John Wiley & Sons.

22. Kee, R. J., Warnatz, J., and Miller, J. A., 1983, Sandia National Laboratories Report, SAND 83- 8209.

23. Kee, R. J., Rupley, F. M., and Miller, J. A., 1987, Sandia National Laboratories Report, SAND 87-8215.

24. Hirata, M., Ohe, S., and Nagahama, K., 1975, Computer-Aided Book of Vapor-Liquid Equilibria, Elsevier.

25. Adewuyi, Y. G., Cho, S. Y., Tsay, R. P., and Carmichael, G. R., 1984, Atmospheric Environment, vol. 18, p. 2413.

26. Norton, T. S., 1990, The Combustion Chemistry of Simple Alcohol Fuels, Ph.D. Thesis, Department of Mechanical and Aerospace Engineering, Princeton University, Princeton, NJ. Report MAE 1877-T.

27. Norton, T. S., and Dryer, F. L., 1990, Toward a Comprehensive Mechanism for Methanol Pyrolysis, Int. Journal Chem. Kin., 22, p. 219.

28. Norton, T. S. and Dryer, F. L., 1989, Some New Observations on Methanol Oxidation Chemistry, Comb. Sci. Tech., 63, p. 107.

29. Egolfopoulos, F. N., Du, D. X., and Law, C. K., 1992, A Comprehensive Study of Methanol Kinetics in Freely-Propagating and Burner-Stabilized Flames, Flow and Static Reactors, and Shock Tubes, Comb. Sci. and Tech., 83, p. 33.

30. Grotheer, H. H., Kelm, H. H., Driver, H. S. T., Hutcheon, R. J., Lockett, R. D., and Robertson, G. N., 1992, Elementary Reactions in the Methanol Oxidation System. Part I: Establishment of the Mechanism and Modeling of Laminar Burning Velocities. Part II.: Measurement and Modeling of Autoignition in a Methanol-Fuelled Otto Engine, Berichte der Bunsengesellschaft.

31. Held, T. J., 1993, The Oxidation of Methanol, Isobutene, and Methyl Tertiary-butyl Ether, Ph.D. Thesis, Department of Mechanical and Aerospace Engineering, Princeton University, Princeton, NJ.

32. Held, T. J., and Dryer, F. L., 1994, An Experimental and Computational Study of Methanol Oxidation in the Intermediate and High Temperature Regimes, Submitted to the Twenty Fifth (International) Symposium on Combustion, Irvine, CA.

33. Choi, M. Y., Dryer, F. L., and Haggard, J. B., Jr., 1989, Some Further Observations on Microgravity Droplet Combustion In the NASA-Lewis Drop Tower Facilities, American Institute of Physics Conference Proceedings, 197, p. 338.

34. Naegeli, D. W., 1989, Combustion-Associated Wear in Alcohol-Fueled Spark Ignition Engines, SAE Technical Paper Series #891641.

35. Stein, Y. S., Choi, M. Y., Cho, S. Y., and Dryer, F. L., 1990, Absorption of Intermediates In Liquid Phase Combustion, Poster Session presented at the Twenty-Third Symposium (International) on Combustion.

36. Lee, A. and Law, C. K., 1991, An Experimental Investigation on the Vaporization and Combustion of Methanol and Ethanol Droplets, Combustion and Flame, 86, pp. 253-265.

37. Law, C. K. 1982, Recent Advances in Droplet Vaporization and Combustion, Progress in Energy and Combustion Science 8, 3, p. 169-199.

38. Cho, S. Y., Personal Communication, 1993.

39. Tyn, M.T. and Calus, W.F., Diffusion Coefficients of Dilute Binary Liquid Mixtures, 1975, Journal of Chemical Engineering Data, 20:106.

40. Law, C. K. and Williams, F. A., 1972, Kinetics and Convection in the Combustion of Alkane Droplets, Combustion and Flame, 19, p. 393.

41. Kumagai, S., Sakai, T., and Okajima, S., 1971, Thirteenth Symposium (International) on Combustion, The Combustion Institute, p. 1139.

42. Shaw, B. D., Dryer, F. L., Williams, F. A. and Haggard, J. B., Jr., 1988, Sooting And Disruption In Spherically-Symmetrical Combustion Of Decane In Air, Acta Astronautica, 17, p. 1195.

43. Choi, M. Y., Dryer, F. L., and Haggard, J. B., Jr., 1991, Observations of A Slow Burning Regime for Hydrocarbon Droplets, Twenty Third Symposium (International) on Combustion, The Combustion Institute, p. 1597.

44. Yang, J. C., Jackson, G. S., and Avedesian, C. T., 1989, Some Experiments on Free Droplet Combustion at Low Gravity, American Institute of Physics Conference Proceedings, 197, p. 394.

45. Jackson, G. S. and Avedisian, C. T., 1991, Possible Effects of Initial Diameter in Spherically Symmetric Droplet Combustion of Sooting Fuels, Fall Eastern States Technical Meeting, The Combustion Institute, Ithaca, NY, November, 1991.

46. Shaw, B. D. and Williams, F. A., 1990, Theory of Influence of a Low-Volatility, Soluble Impurity on Spherically-Symmetric Combustion of Fuel Droplets, International Journal of Heat and Mass Transfer 33, pp. 301-317.

47. Weinberg, F., 1991, personal communications.

48. Parks, G. S. and Huffman, H. M., 1930, J. Am. Chem. Soc., 52, p. 1032.

49. Warnatz, J., 1984, Chemistry of High Temperature Combustion of Alkanes up to Octane, Twentieth Symposium (International) on Combustion, The Combustion Institute, p. 845.

50. Bui-Pham, M. and Sheshadri, K., 1991, Comparison Between Experimental Measurements and Numerical Calculations of the Structure of n-Heptane-air Diffusion Flames, Comb. Sci. and Tech., 79, p. 293.

51. Kent, J. H. and Williams, F. A., 1974, Extinction of Laminar Diffusion Flames for Liquid Fuels, Fifteenth Symposium (International) on Combustion, The Combustion Institute, p. 315.

52. Kennedy, S, Brezinsky, K. and Dryer, F., 1985, Flow Reactor Oxidation Studies of the Extent of Reaction in Heptane/Iso-octane Mixtures as a Function of Octane Number, Eastern Sectional Meeting of the Combustion Institute, Philadelphia, PA, 1985. Also Kennedy, S. BSE Thesis, Dept. of Chemical Engineering, Princeton University, Princeton, NJ, 1986.

53. Law, C. K. and Chung, S. H., 1986, An Experimental Study of Droplet Extinction in the Absence of External Convection, Combustion and Flame, 64, p. 237.

54. Randolph, A. L. and Law, C. K., 1986, Influence of Physical Mechanisms on Soot Formation and Destruction in Droplet Burning, Combustion and Flame, 64, p. 267.

FIGURES

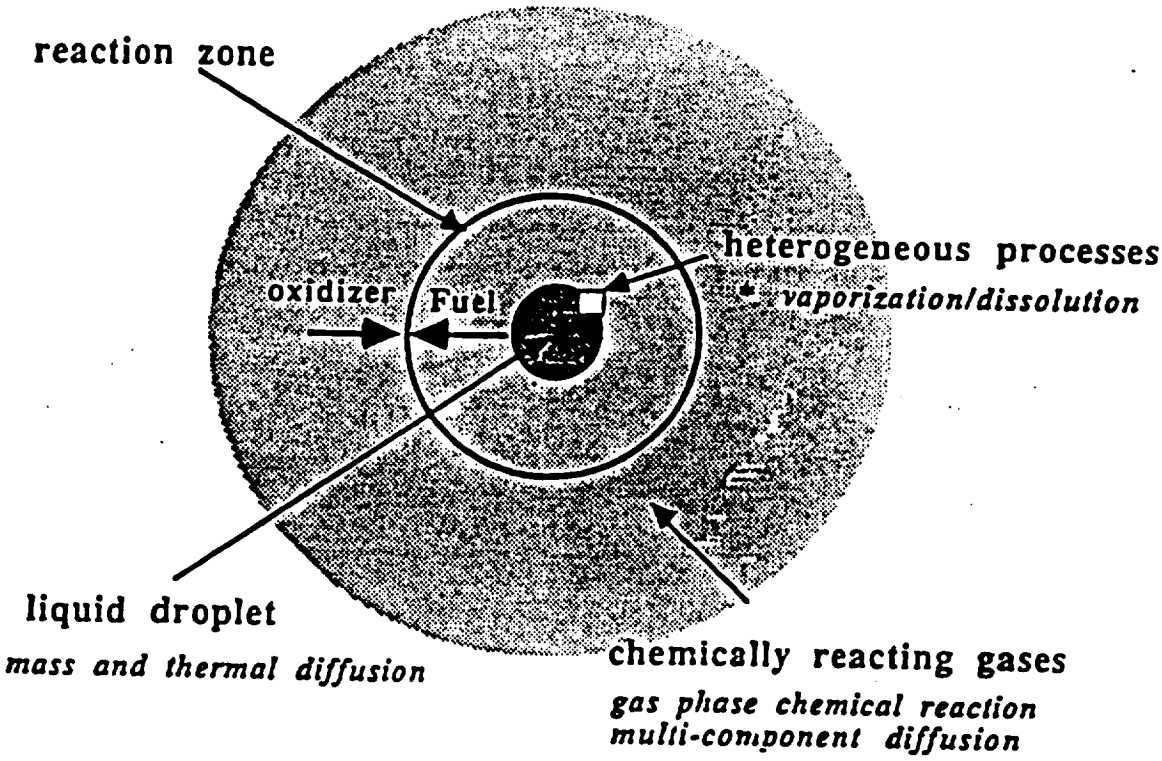

Figure 1. Schematic Diagram of Sphere-symmetric Detailed Modeling of Droplet Combustion.

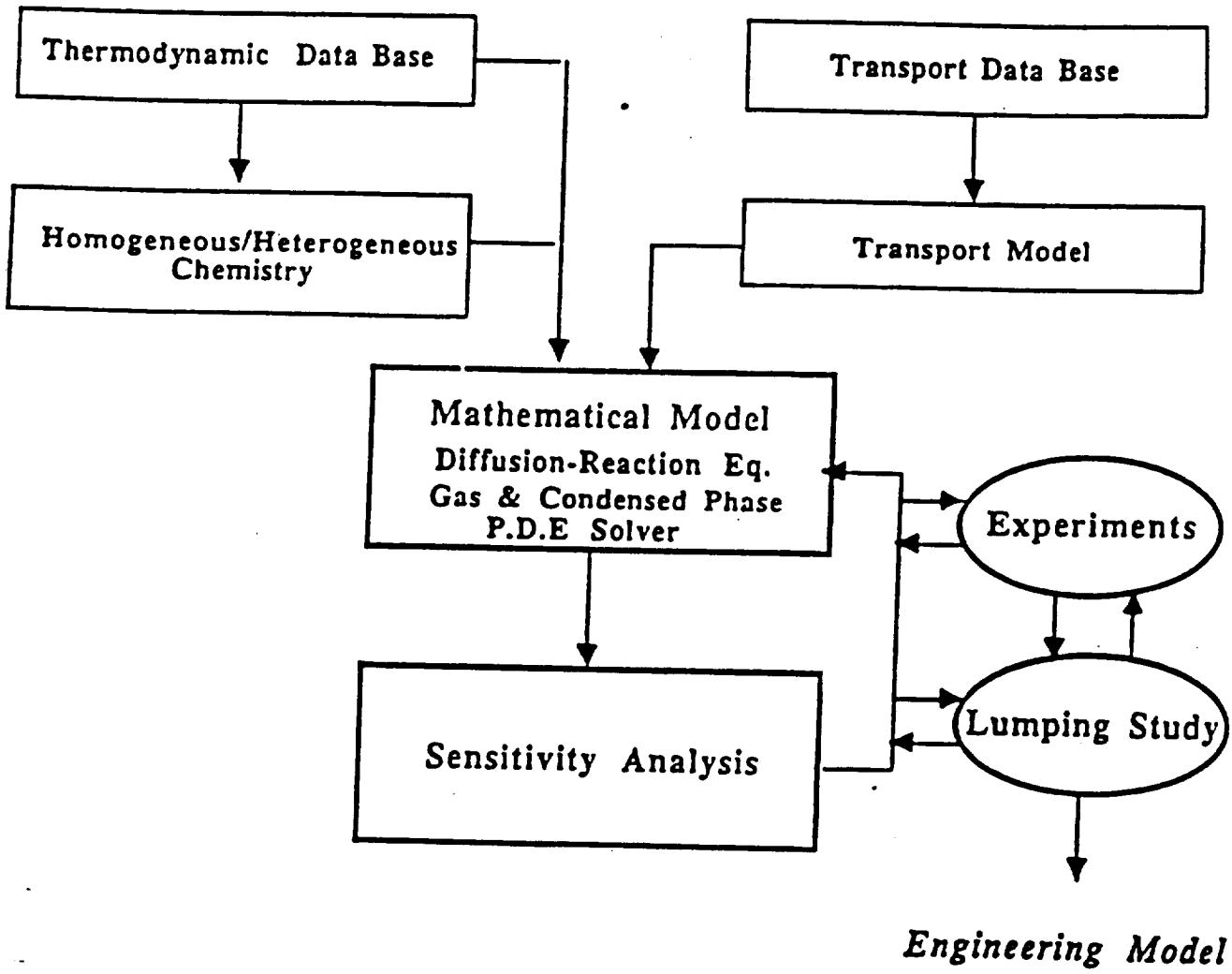

Figure 2. Schematic Diagram of Computational Modeling Approach.

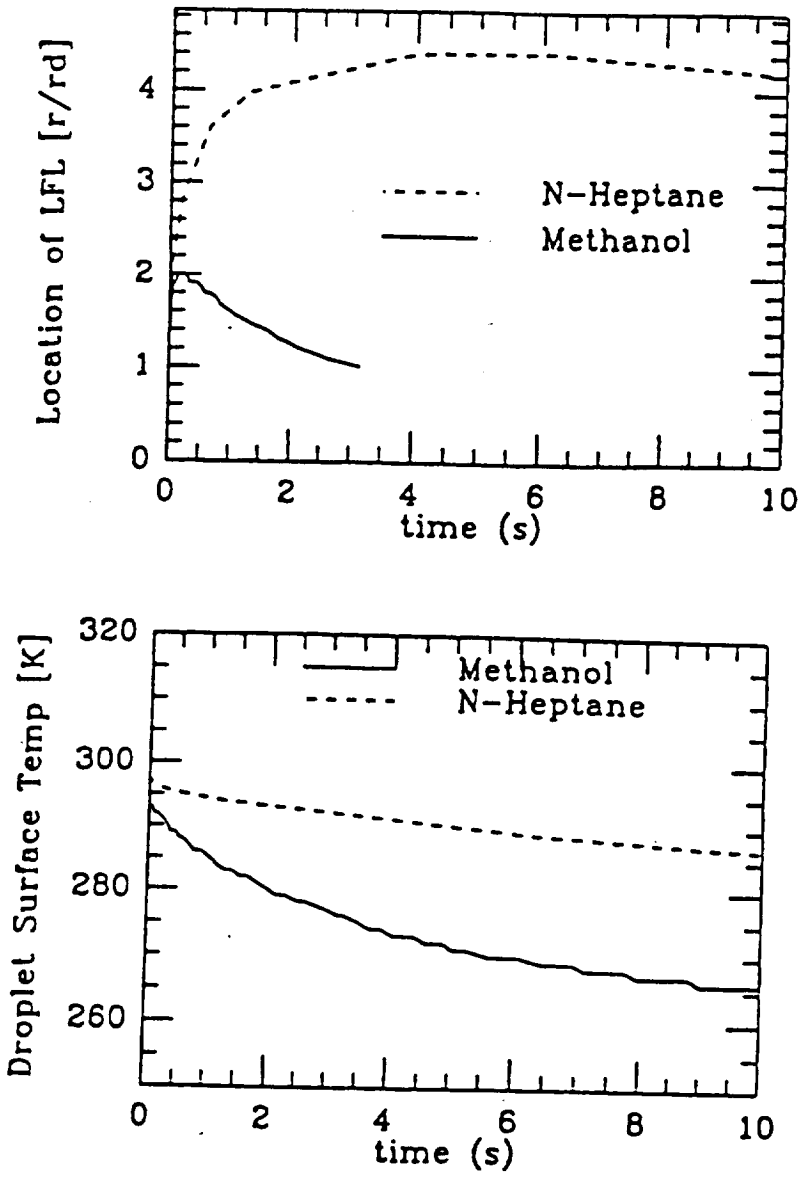

Figure 3. Vaporization Modeling Results for Methanol and N-Heptane Droplets at One Atmosphere Pressure. Initial Droplet Diameter, 1.6 mm.; Initial Droplet and Ambient Temperature, 298 K; 0% Humidity. (From Ref. 17).

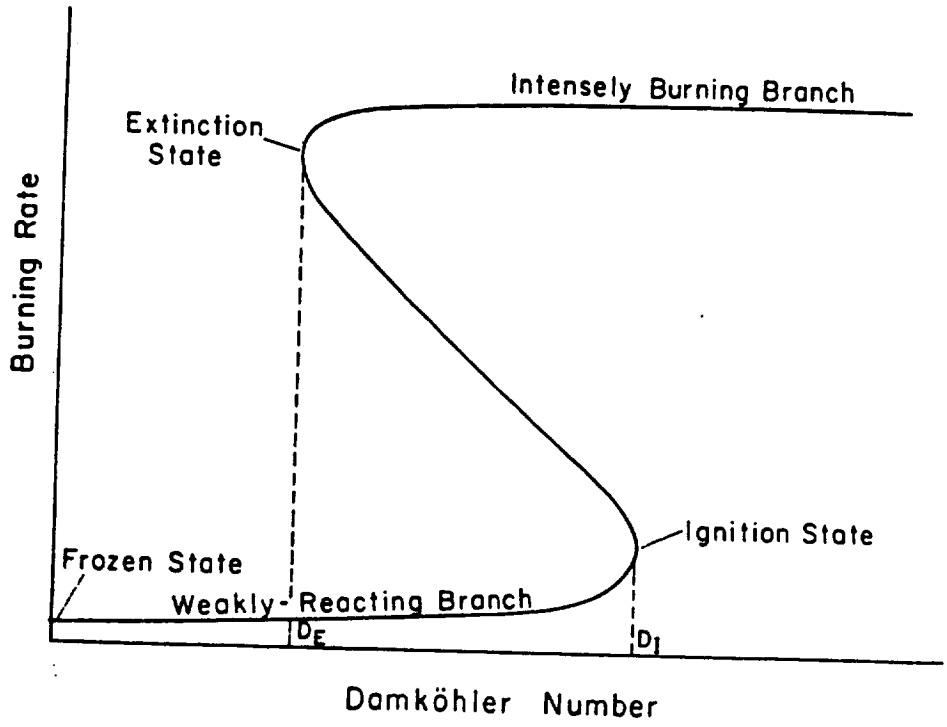

Figure 4. Gasification rate S-curve showing all possible steady state solutions for droplet combustion and vaporization. (From Ref. 37)

a) Deployment of Droplet & Ignition Source

* *fuel vaporization*
* *intense droplet heating*

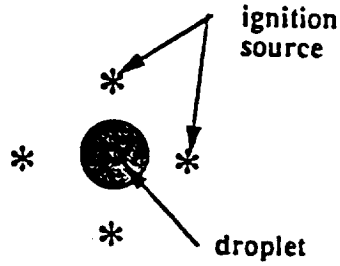

b) Droplet ignition & Unsteady Burning

* *development of diffusion flame*
* *intense droplet heating*
* *flame expansion*

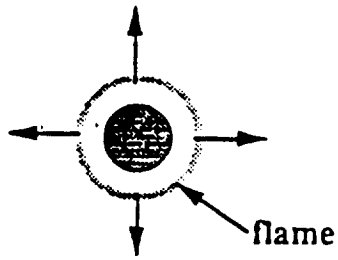

c) Quasi-steady Burning

* *constant burning rate*
* *constant flame stand-off ratio*

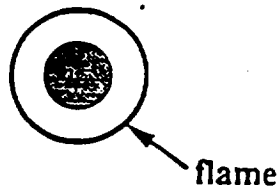

fast chemical reaction

d) Droplet Extinction

* *sharp decrease in the burning rates*

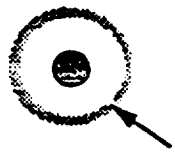

flame extinguishment

fast heat transport in the gas phase

Figure 5. Physical Process Schematic for Sphere-symmetric Droplet Burning. a) Deployment of Droplet & Ignition Source; b) Droplet Ignition and Unsteady Burning; c) Quasi-steady Burning; d) Droplet Extinction.

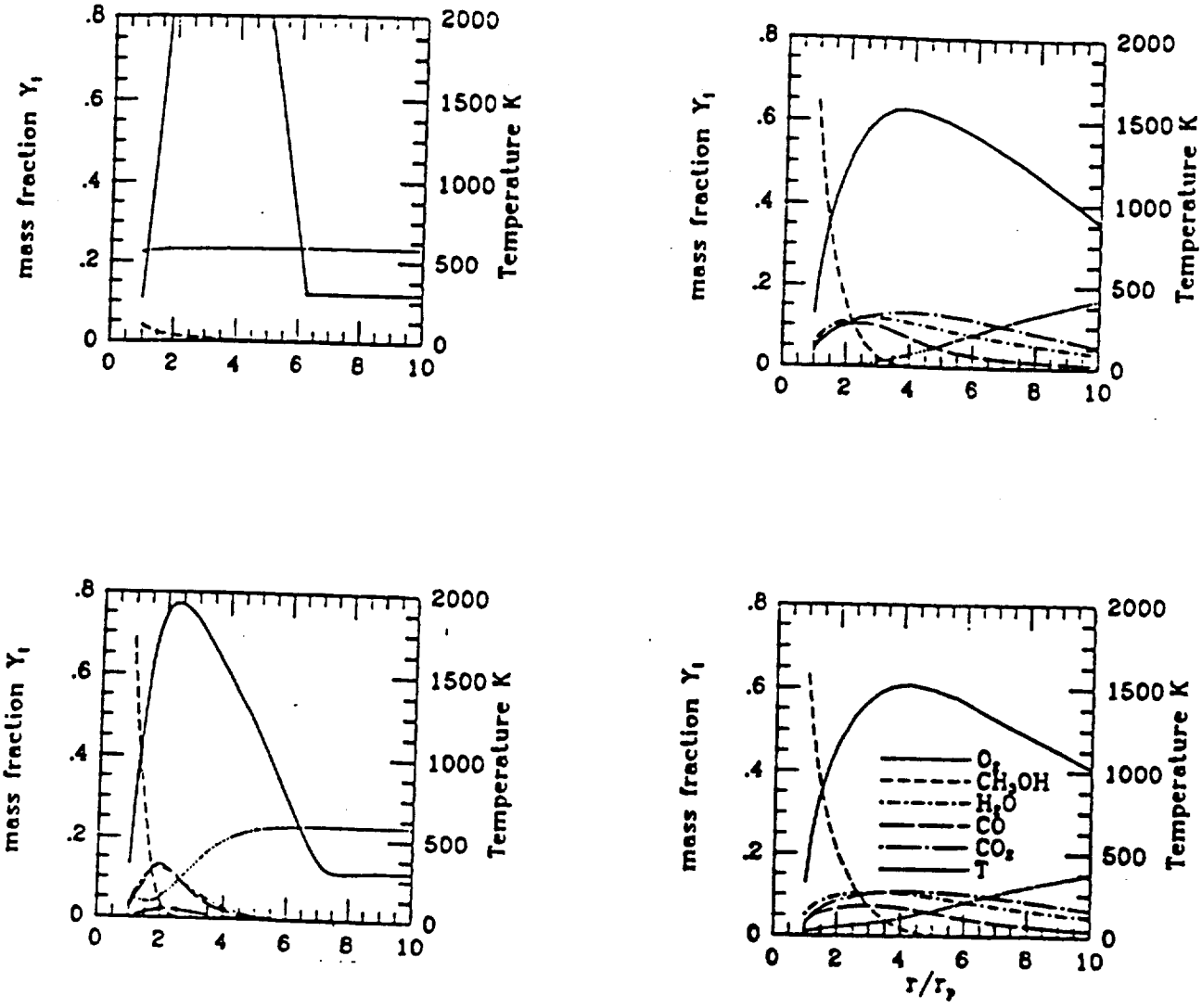

Figure 6. Typical Numerical Modeling Characteristics for Methanol Droplet Combustion Corresponding to Processes Depicted in Figure A4. Mass Fraction of Major Gas-Phase Species and Temperature as Functions of Non-dimensional particle Radius for a) Initial State at Application of Ignition Source; b) Ignition; c) Quasi-steady Combustion; d) Extinction.

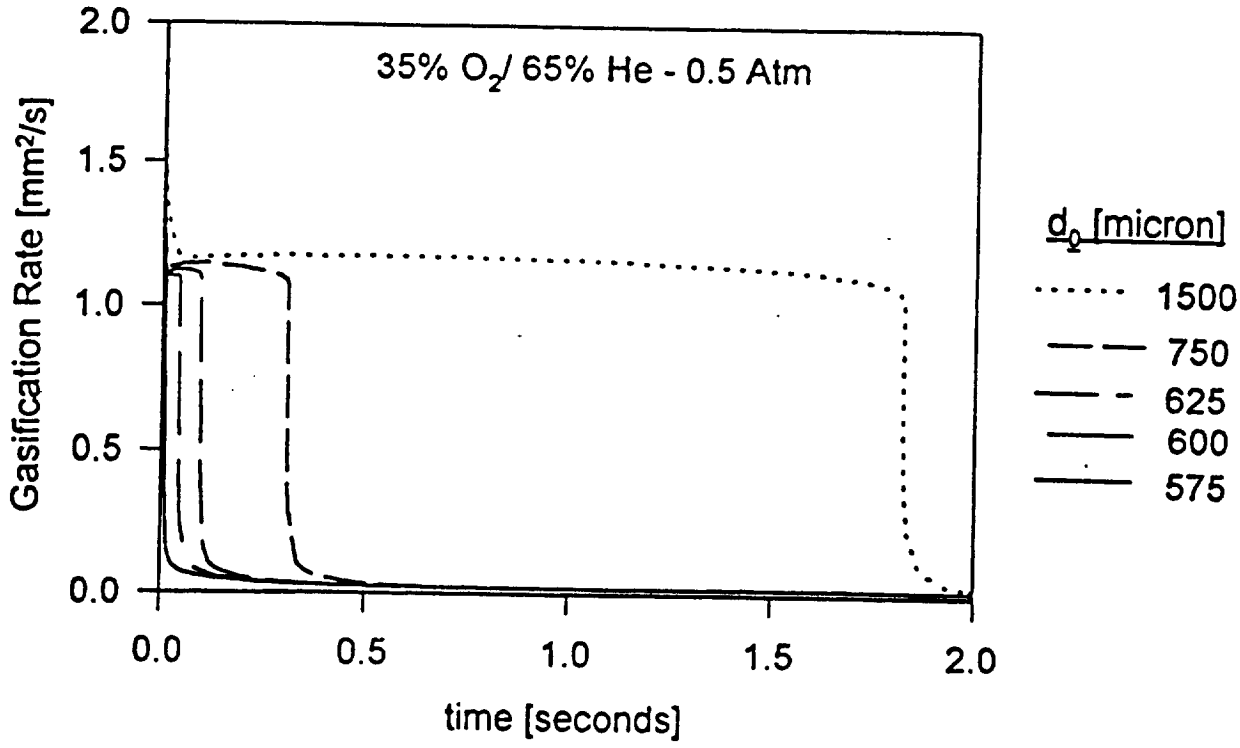

Figure 7. Instantaneous Gasification Rate as a Function of Initial Droplet Diameter for the Same Initial Ambient and Ignition Source Conditions.

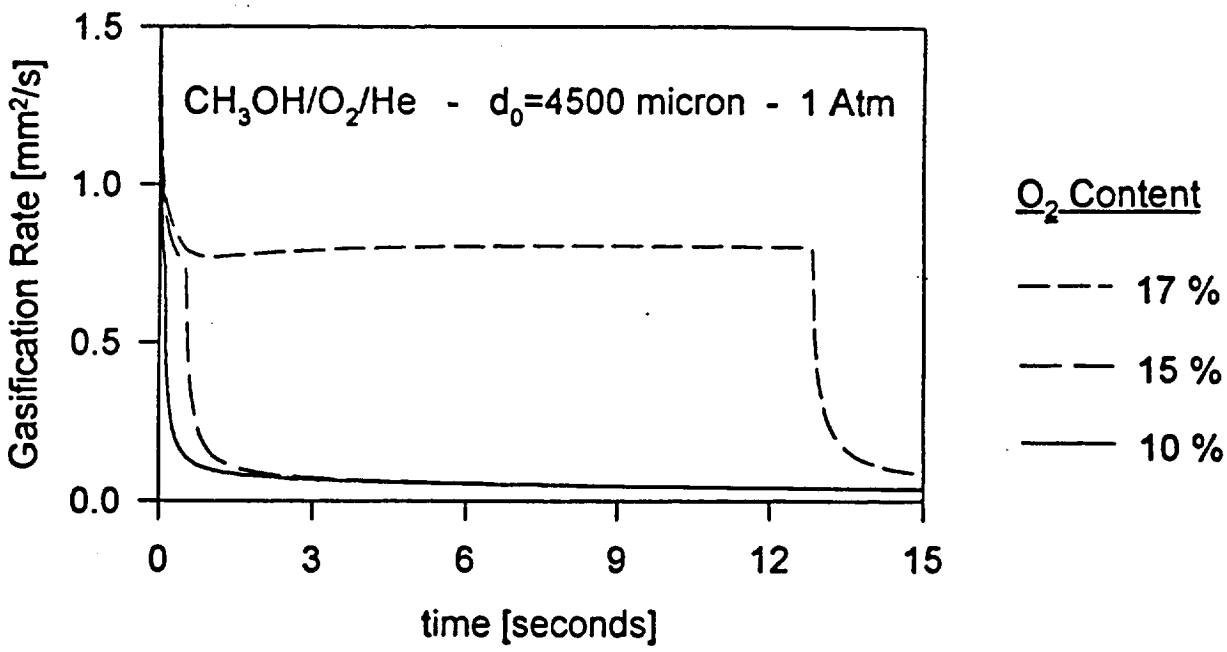

Figure 8. Instantaneous Gasification Rate as a Function of Oxygen Index for the Same Initial Droplet Diameter, Pressure, and Ignition Source Conditions.

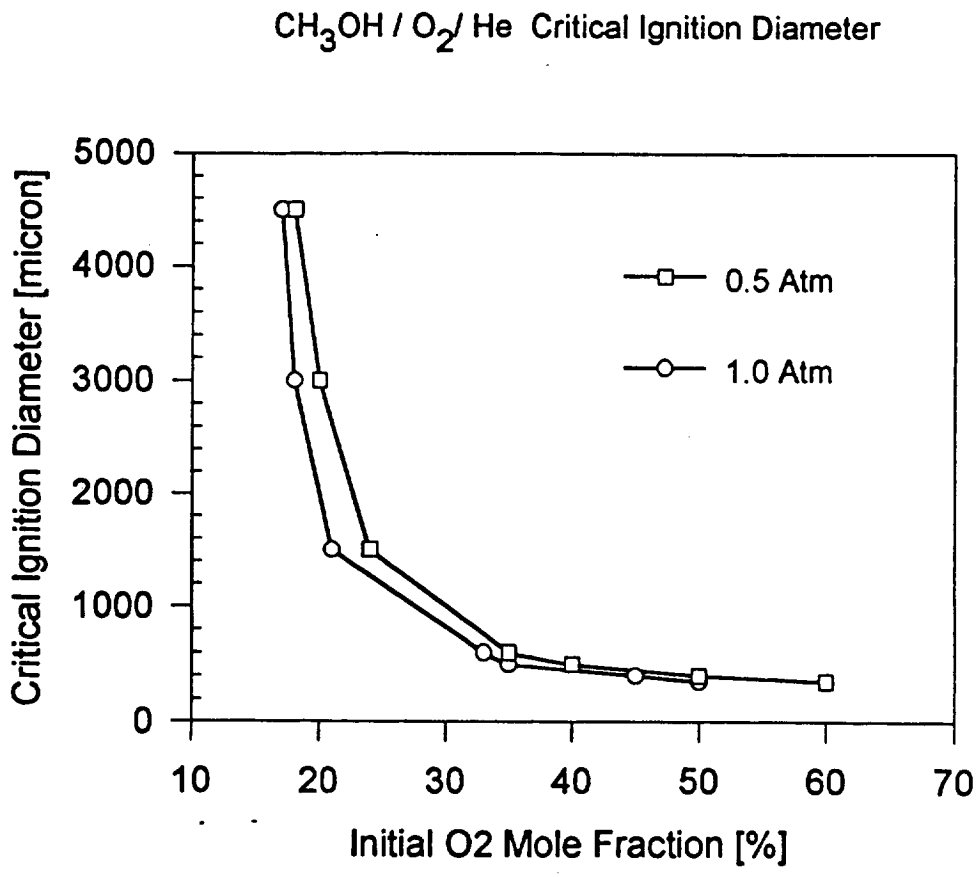

Figure 9. Critical Ignition Diameter for Methanol Droplets in Helium/Oxygen Mixtures as a Function of Oxygen Index and Ambient Pressure.

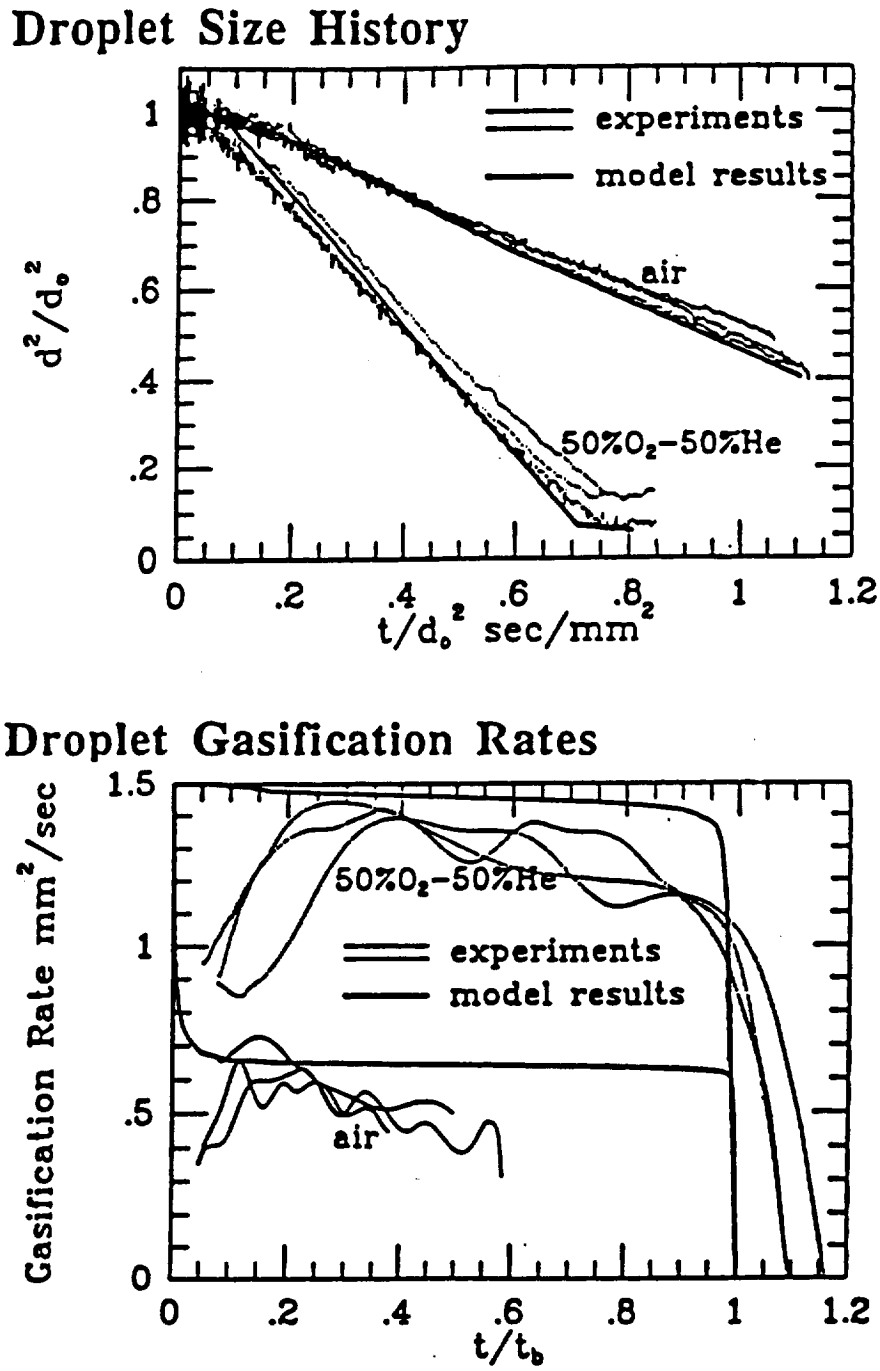

Figure 10. Combustion Behavior of Methanol Droplets (NASA LeRC 2.2 Second Drop tower) in 50%/50% Helium-Oxygen Mixtures at One Atmosphere Pressure: a) Square of Droplet Diameter as Function of Time; b) Transient Behavior of Gasification Rate. (From Ref. 10).

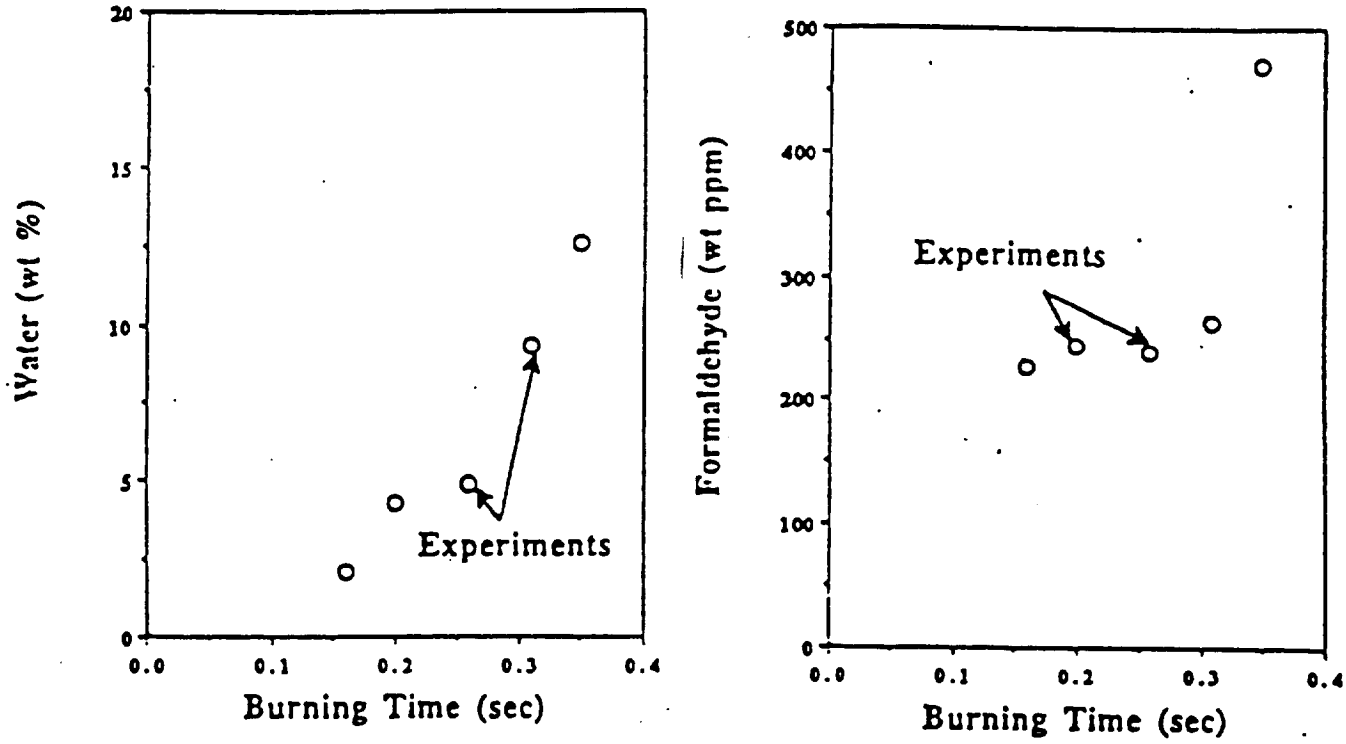

Figure 11. Average Water and Formaldehyde Liquid-Phase Content as a Function of Burning Time for Freely Falling (Initially Pure) Methanol Droplets. Initial Droplet Diameter, 1.5 mm; Ambient Conditions, Pure Oxygen at 298 K and One Atmosphere Pressure. (from Refs. 11, 14).

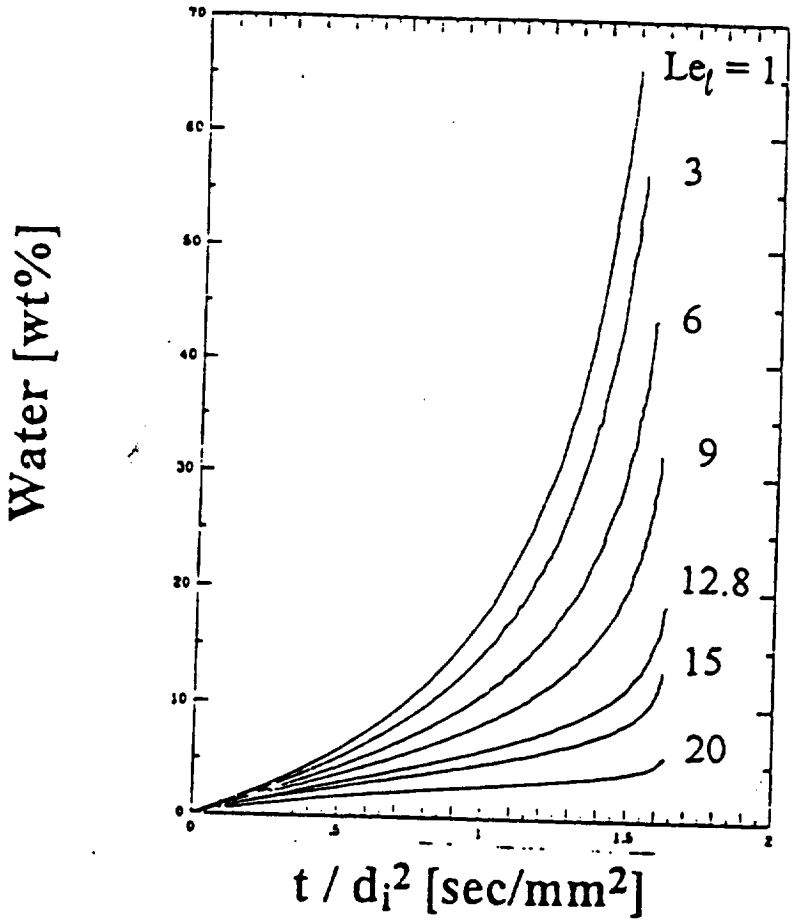

Figure 12. Calculated Average Water Content as a Function of Liquid Phase Lewis Number. Initial Diameter, 1.5 mm; 100% Oxygen at One Atmosphere Pressure.

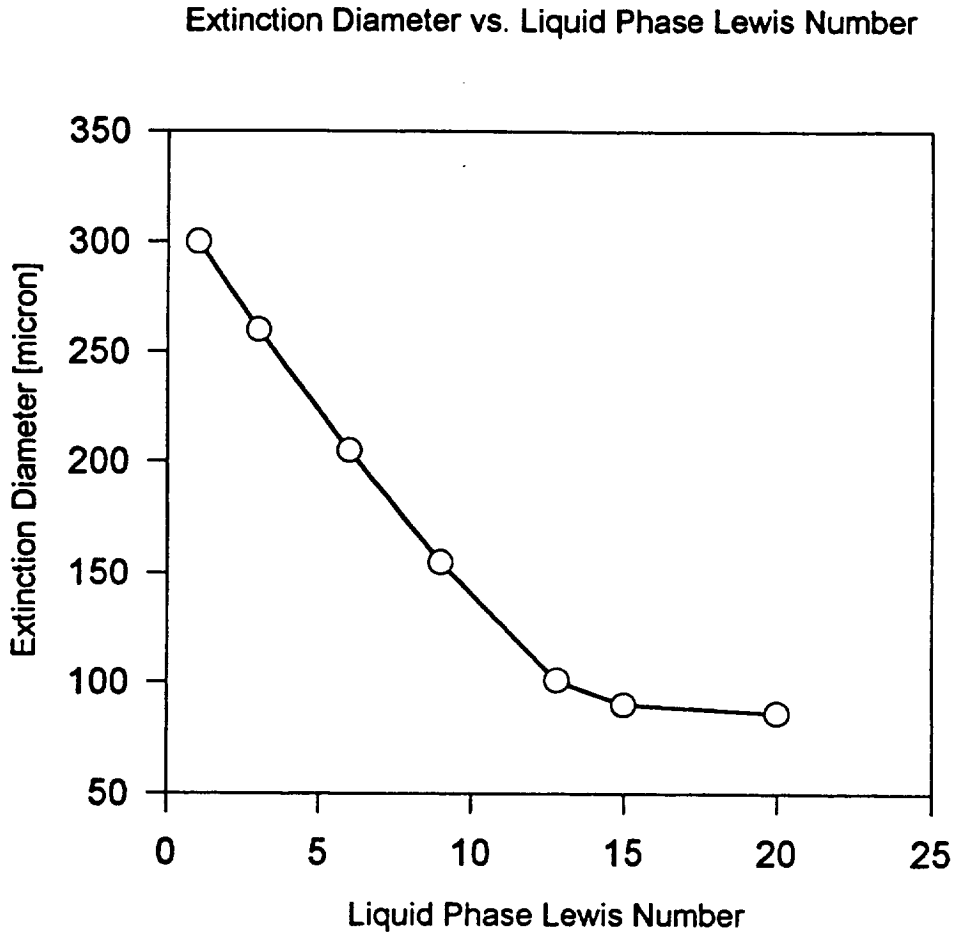

Figure 13. Calculated Extinction Diameter for Initially Pure Methanol Droplets as a Function of Liquid Phase Lewis Number. Initial Diameter, 1.5 mm; 100% Oxygen at One atmosphere Pressure.

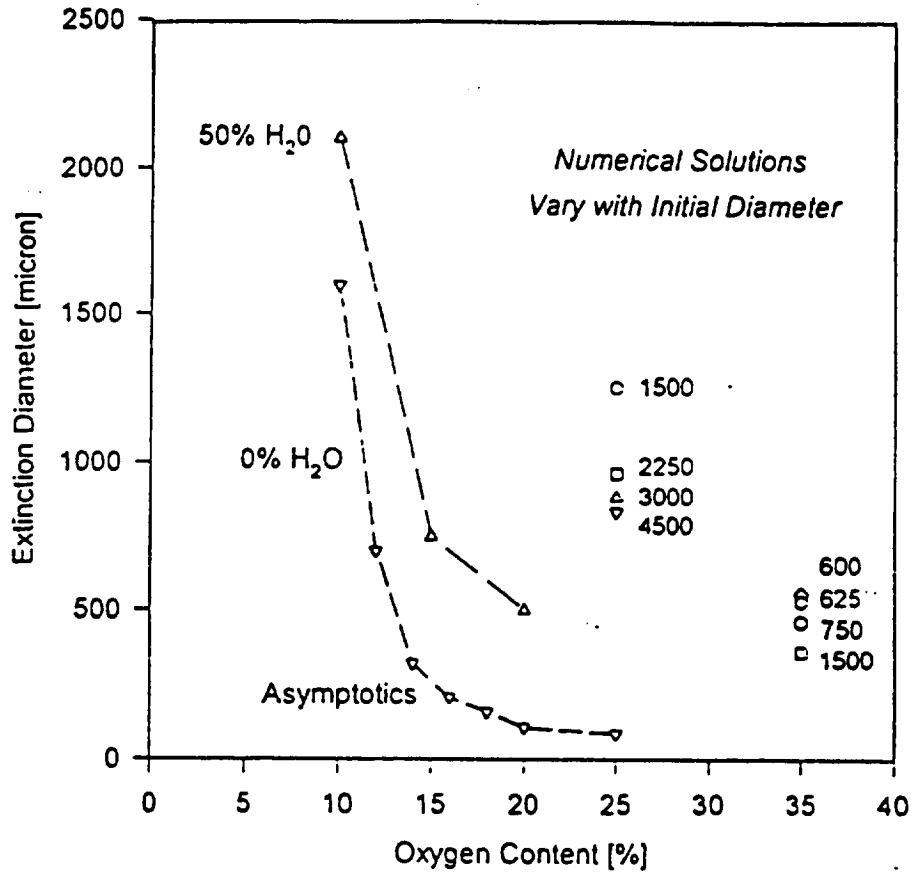

Figure 14. Asymptotic and Numerical Extinction Diameter for Initially Pure Methanol Droplets in Helium/Oxygen Mixtures at One Atmosphere Pressure. Asymptotic Results (Connected by Dashed Lines) for Assumed Average Water Contents (From Ref. 7). Numerical Predictions (Individual Data Points; Adjacent numbers refer to Initial Droplet Diameter.

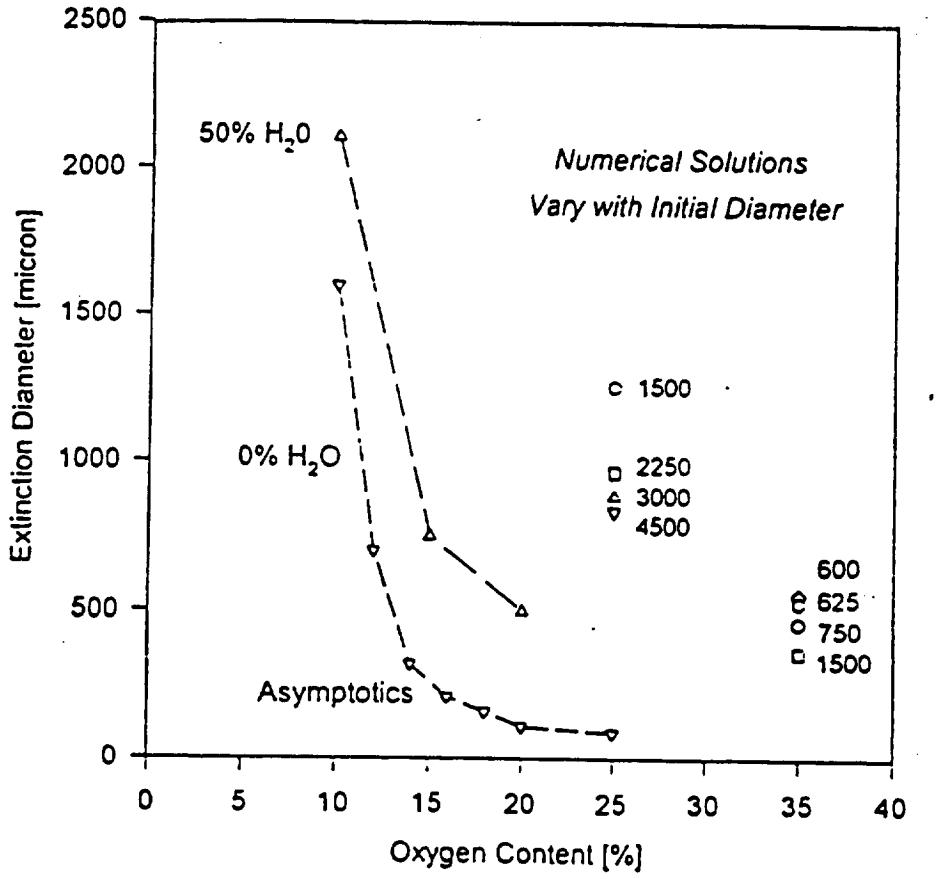

Figure 14. Asymptotic and Numerical Extinction Diameter for Initially Pure Methanol Droplets in Helium/Oxygen Mixtures at One Atmosphere Pressure. Asymptotic Results (Connected by Dashed Lines) for Assumed Average Water Contents (From Ref. 7). Numerical Predictions (Individual Data Points; Adjacent numbers refer to Initial Droplet Diameter.

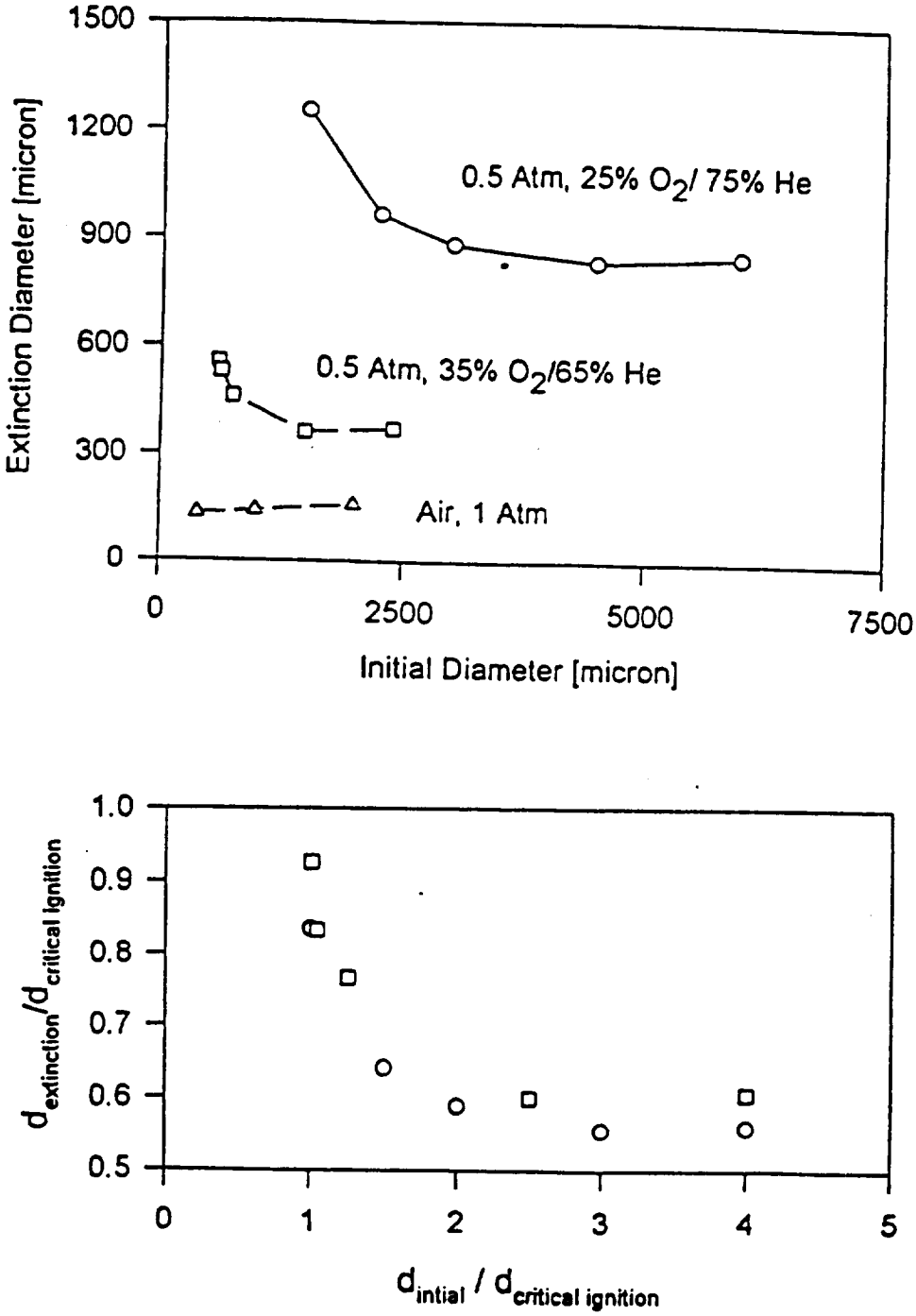

Figure 15. Numerically Calculated Extinction Diameters for Initially Pure Methanol Droplets as a function of Initial Diameter (Other Conditions as Noted).

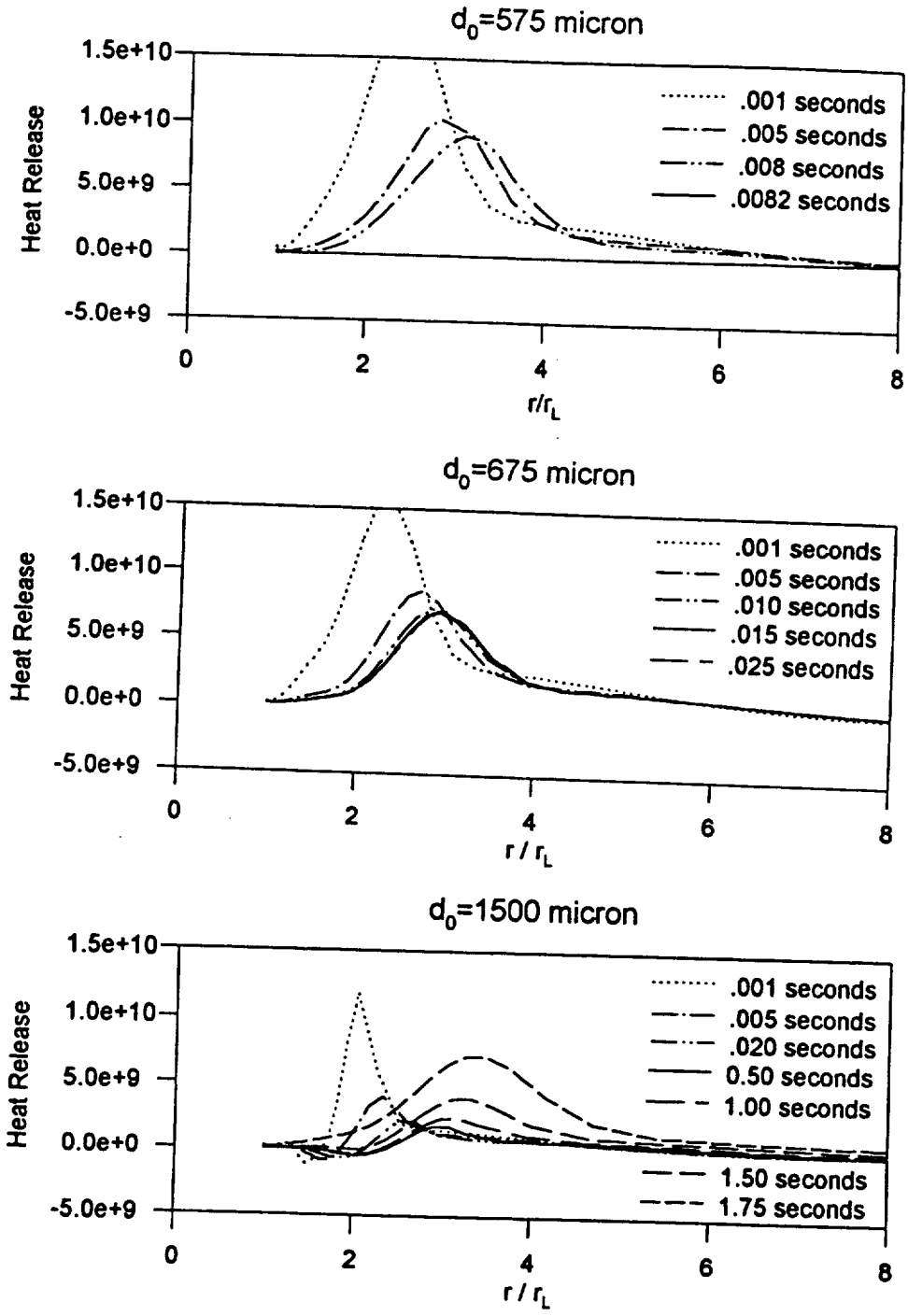

Figure 16. Evolution of gas phase chemical heat release for the combustion of 575, 675, and 1500 micron methanol droplets in 50% He/50% O_2 at 0.5 Atm.

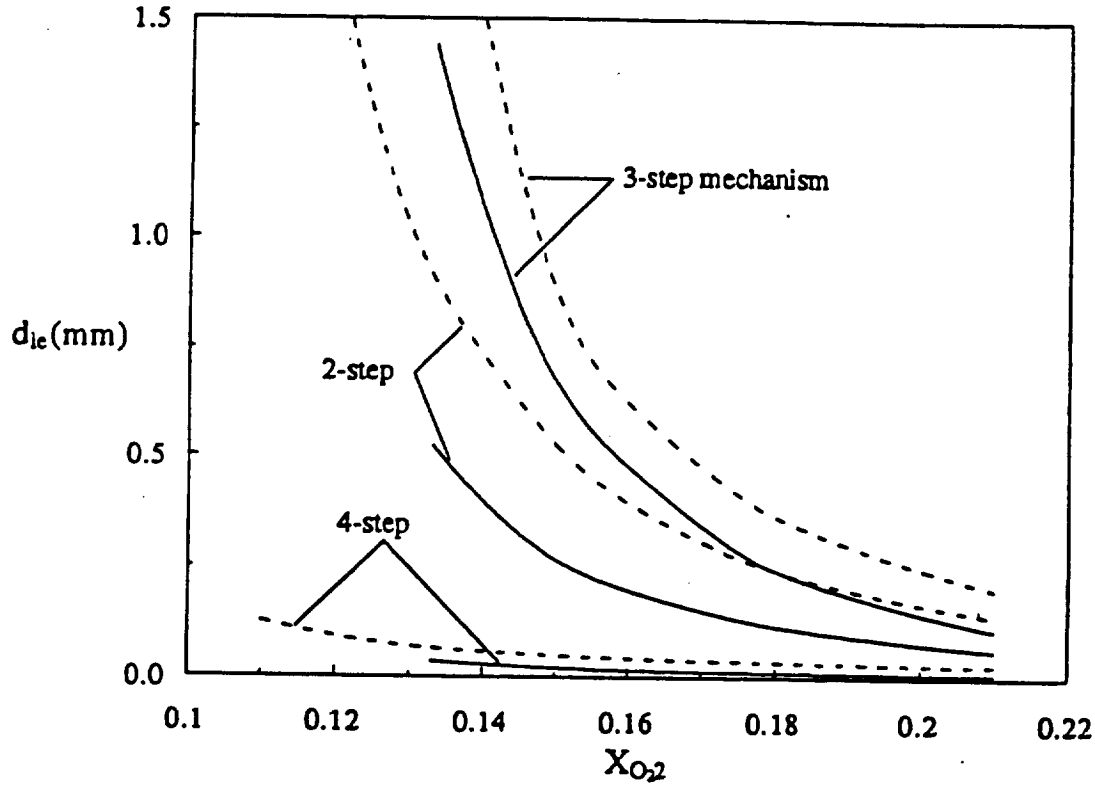

Figure 17. Extinction Diameter for N-Heptane Droplet Combustion in Nitrogen-Oxygen Mixtures Calculated Using Rate-Ratio Asymptotics and Two-, Three- and Four-step Reduced Chemistry. Solid Lines, one Atmosphere Pressure; Dashed Lines, 0.25 Atmospheres Pressure. (From Ref. 5)

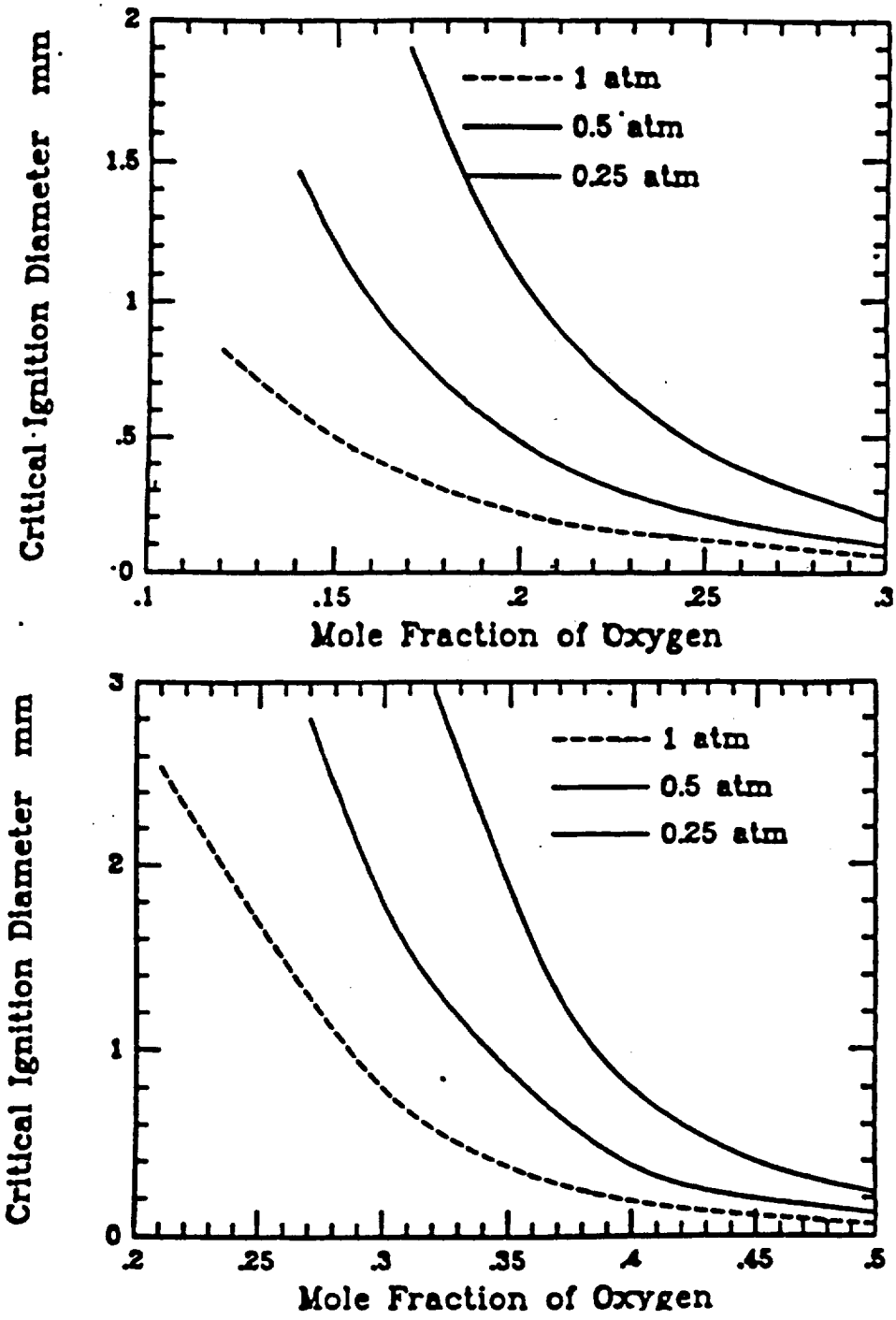

Figure 18. Numerically Calculated Critical Ignition Diameter as a Function of Oxygen indexand Ambient Pressure for N-Heptane Droplet Combustion. a) In Nitrogen-Oxygen Mixtures; b) In Helium-Oxygen Mixtures. (From Ref 12).

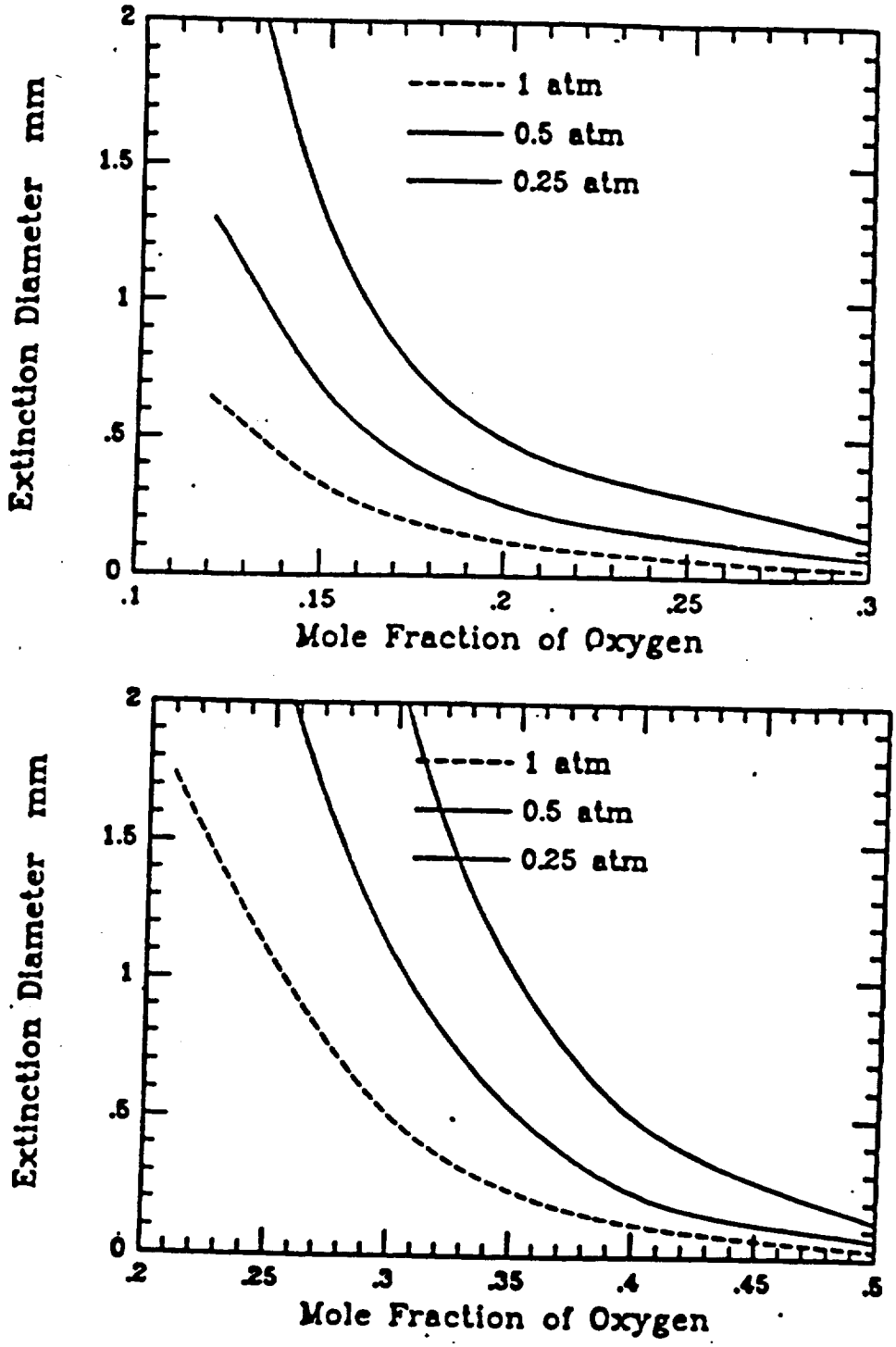

Figure 19. Numerically Calculated Extinction Diameter as a Function of Oxygen index and Ambient Pressure for N-Heptane Droplet Combustion. a) In Nitrogen-Oxygen Mixtures; b) In Helium-Oxygen Mixtures. (From Ref. 12).

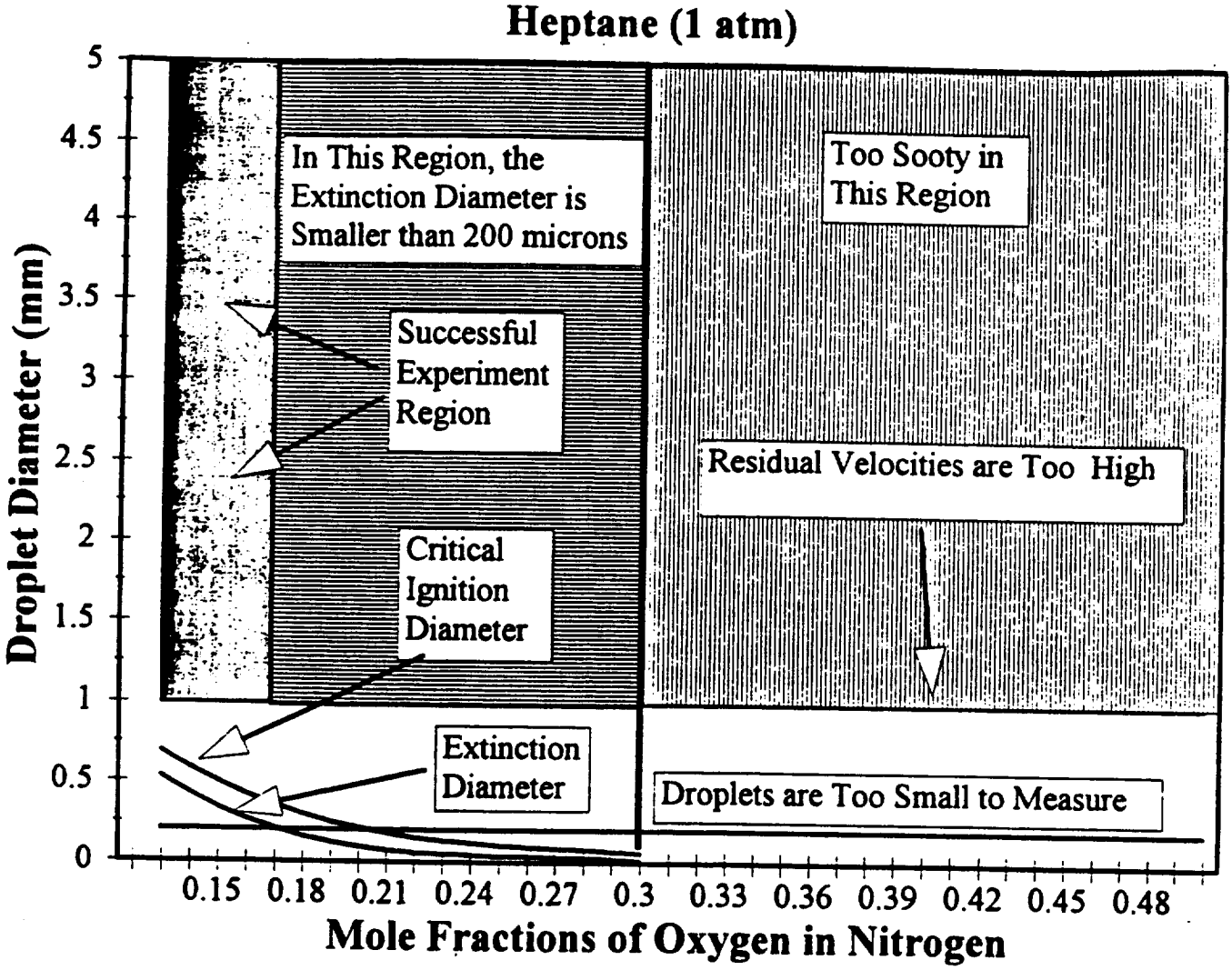

Figure 20. Experimental Test Matrix Envelope for N-Heptane Droplet Combustion in Nitrogen-Oxygen Mixtures at One Atmosphere Pressure.

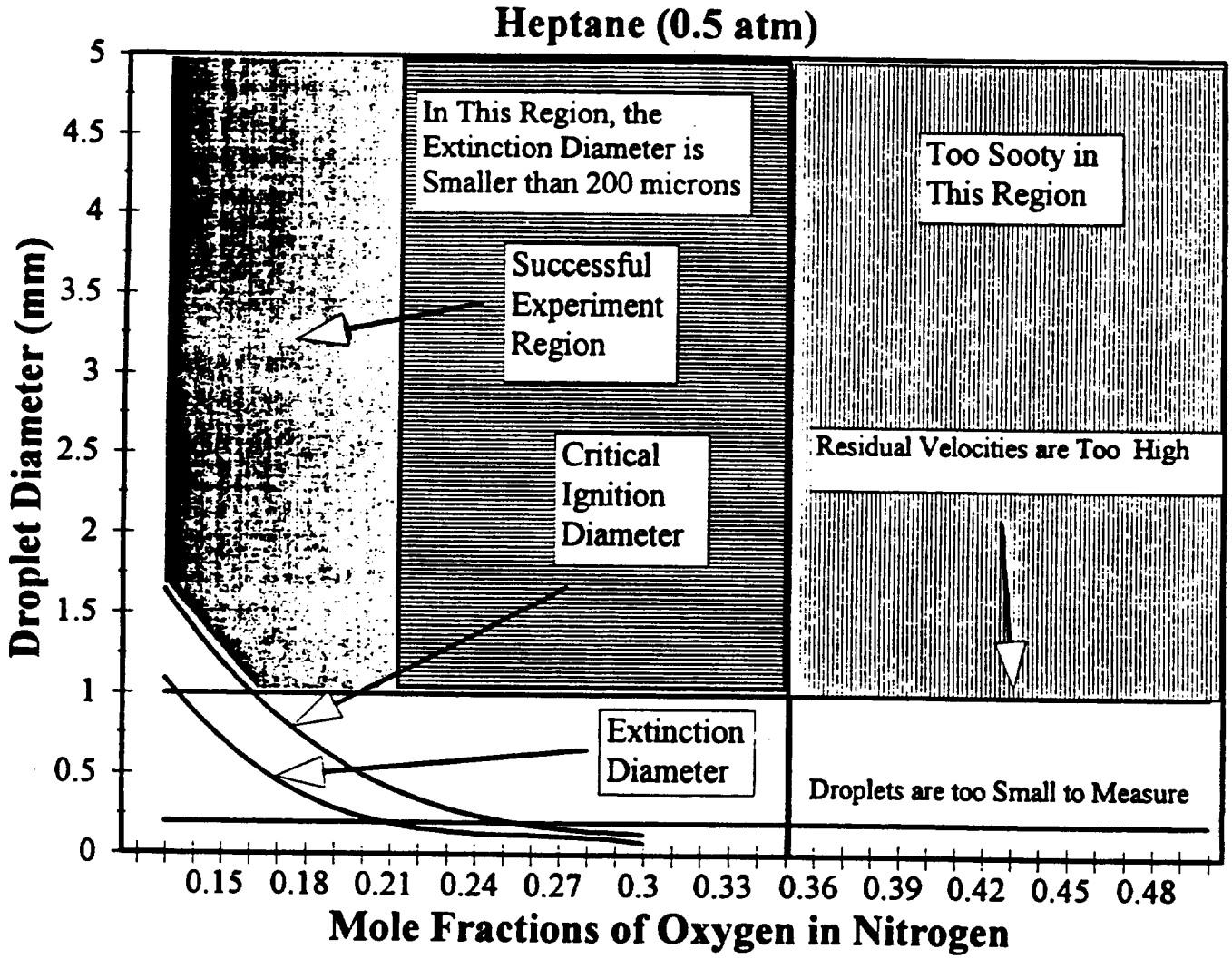

Figure 21. Experimental Test Matrix Envelope for N-Heptane Droplet Combustion in Nitrogen-Oxygen Mixtures at 0.5 Atmospheres Pressure.

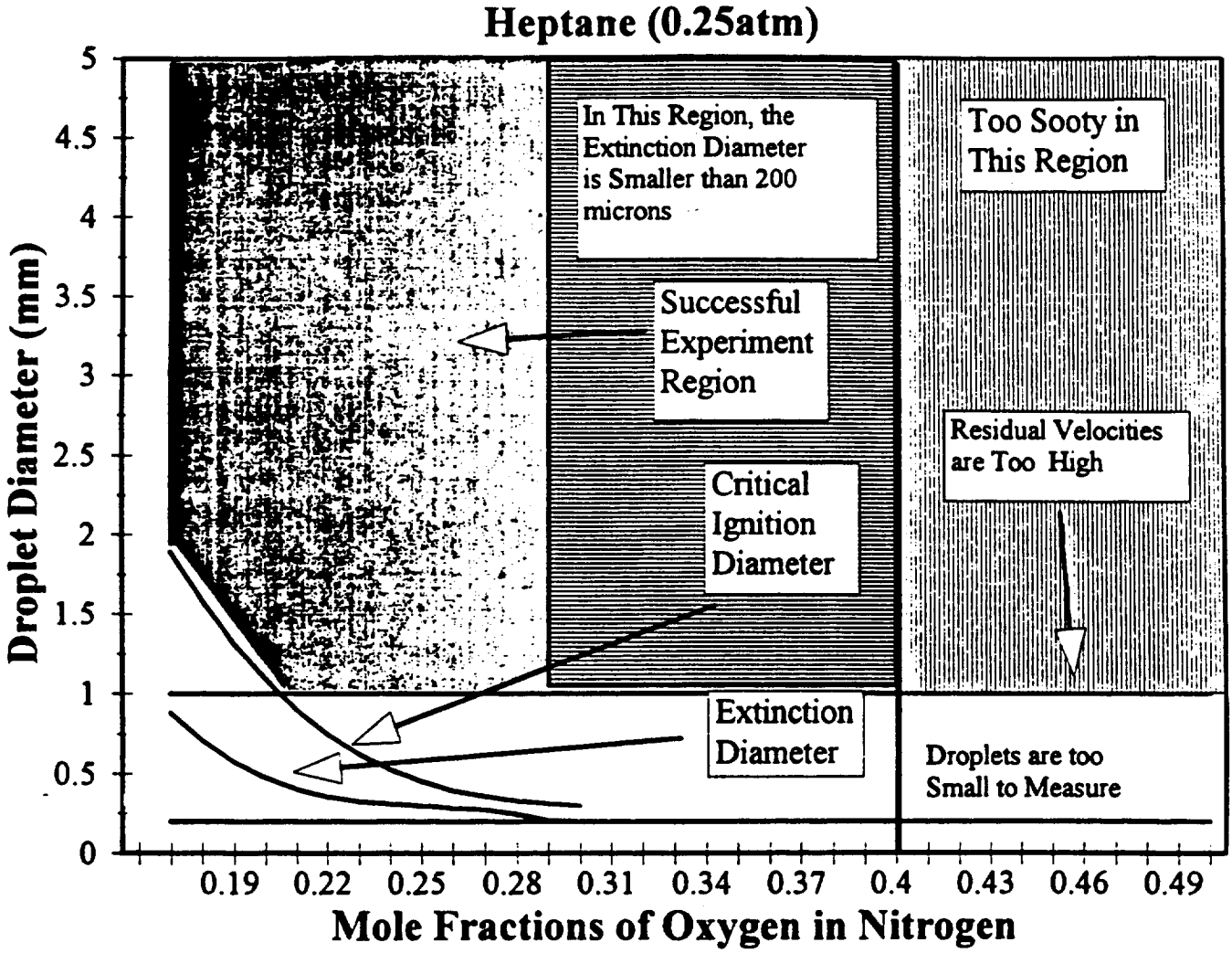

Figure 22. Experimental Test Matrix Envelope for N-Heptane Droplet Combustion in Nitrogen-Oxygen Mixtures at 0.25 Atmospheres Pressure.

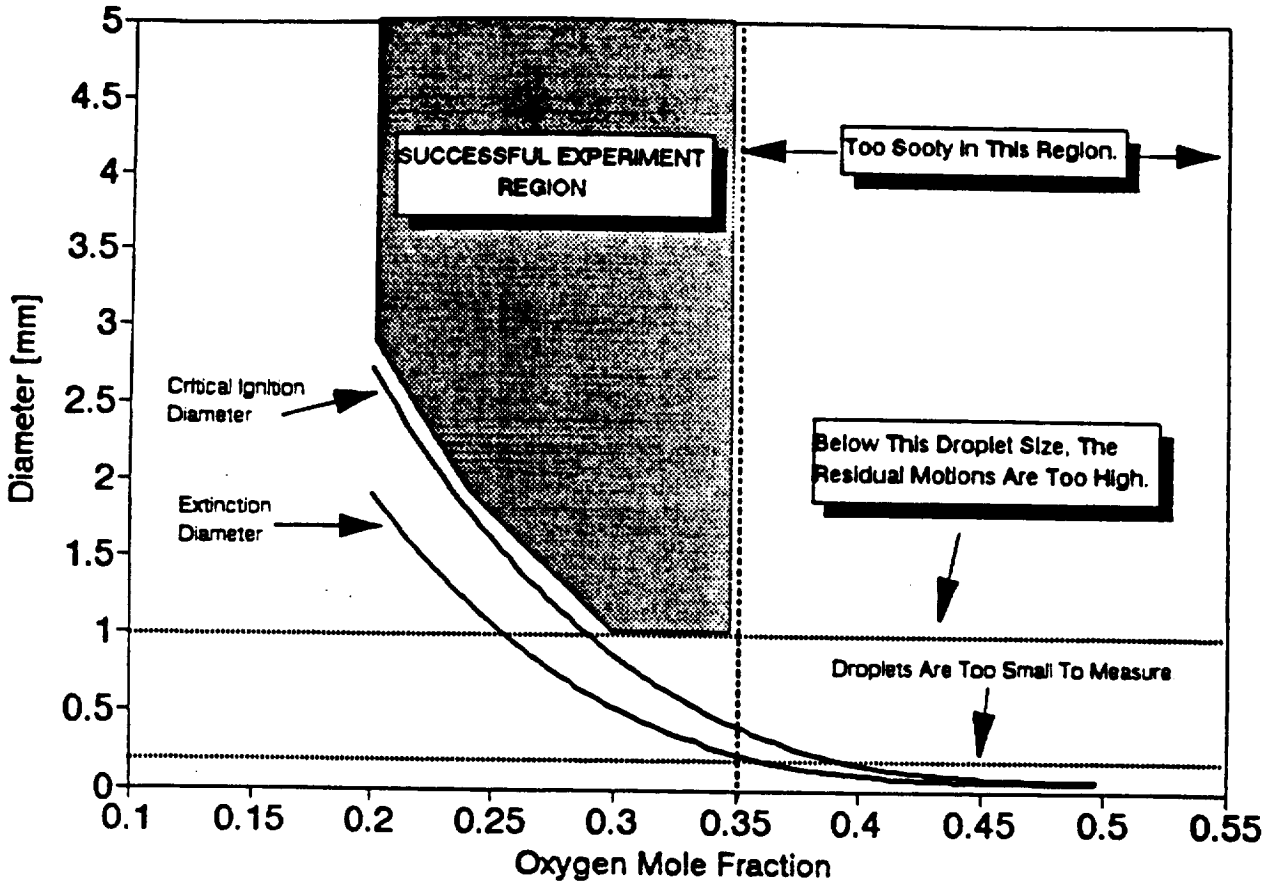

Figure 23. Experimental Test Matrix Envelope for N-Heptane Droplet Combustion in Helium-Oxygen Mixtures at One Atmosphere Pressure. (From Refs. 12, 14, 16).

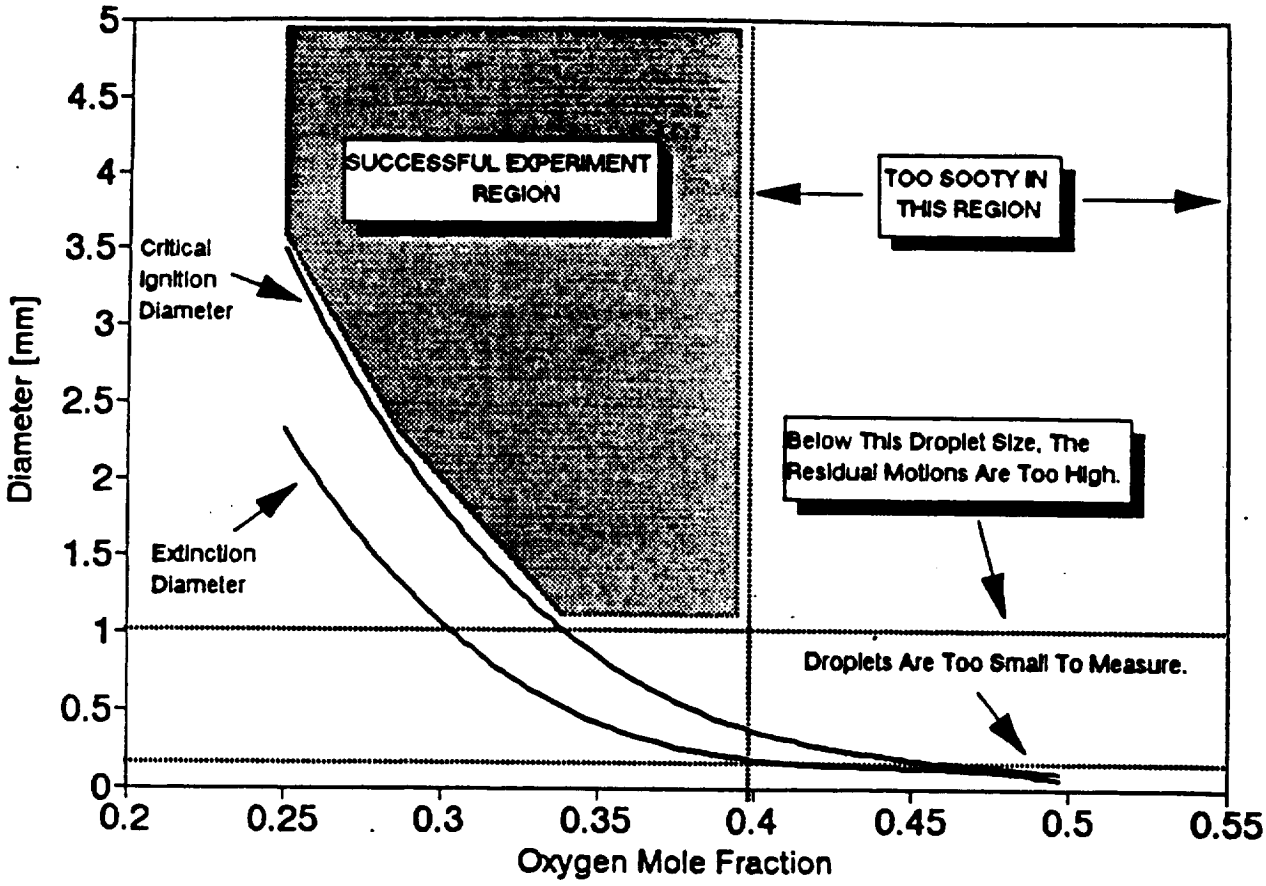

Figure 24. Experimental Test Matrix Envelope for N-Heptane Droplet Combustion in Helium-Oxygen Mixtures at 0.5 Atmospheres Pressure. (From Refs. 12, 14, 16).

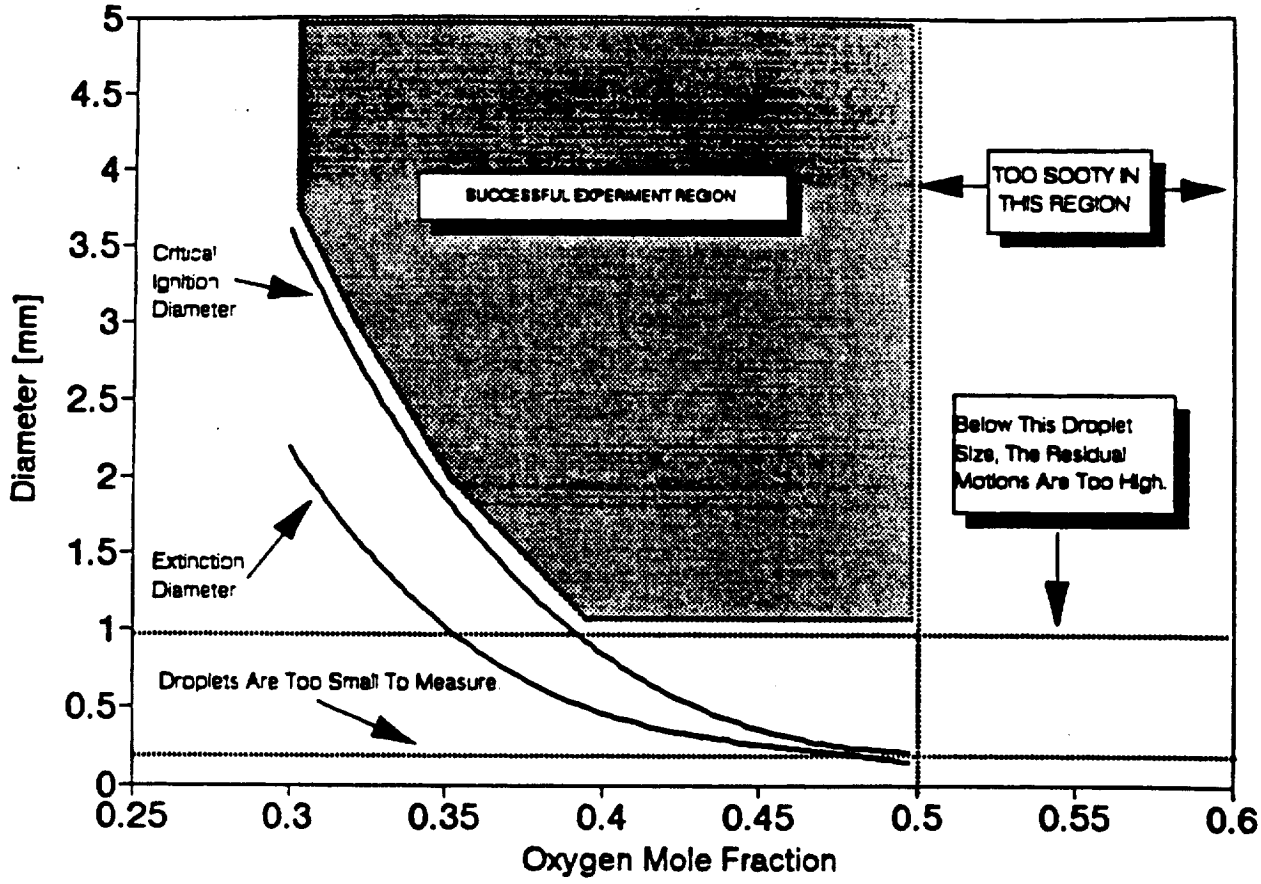

Figure 25. Experimental Test Matrix Envelope for N-Heptane Droplet Combustion in Helium-Oxygen Mixtures at 0.25 Atmospheres Pressure. (From Refs. 12, 14, 16).

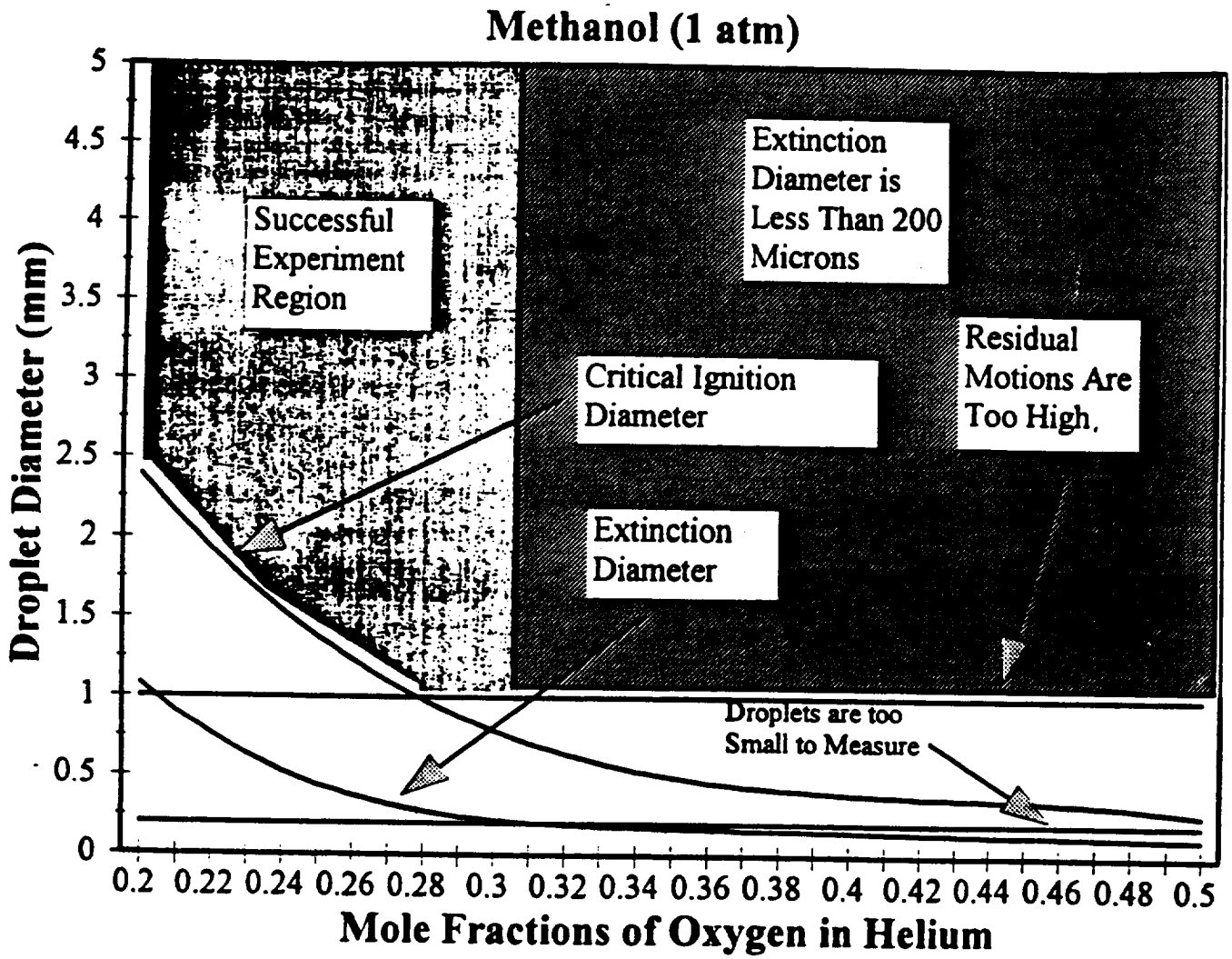

Figure 26. Experimental Test Matrix Envelope for Methanol Droplet Combustion in Helium-Oxygen Mixtures at One Atmosphere Pressure.

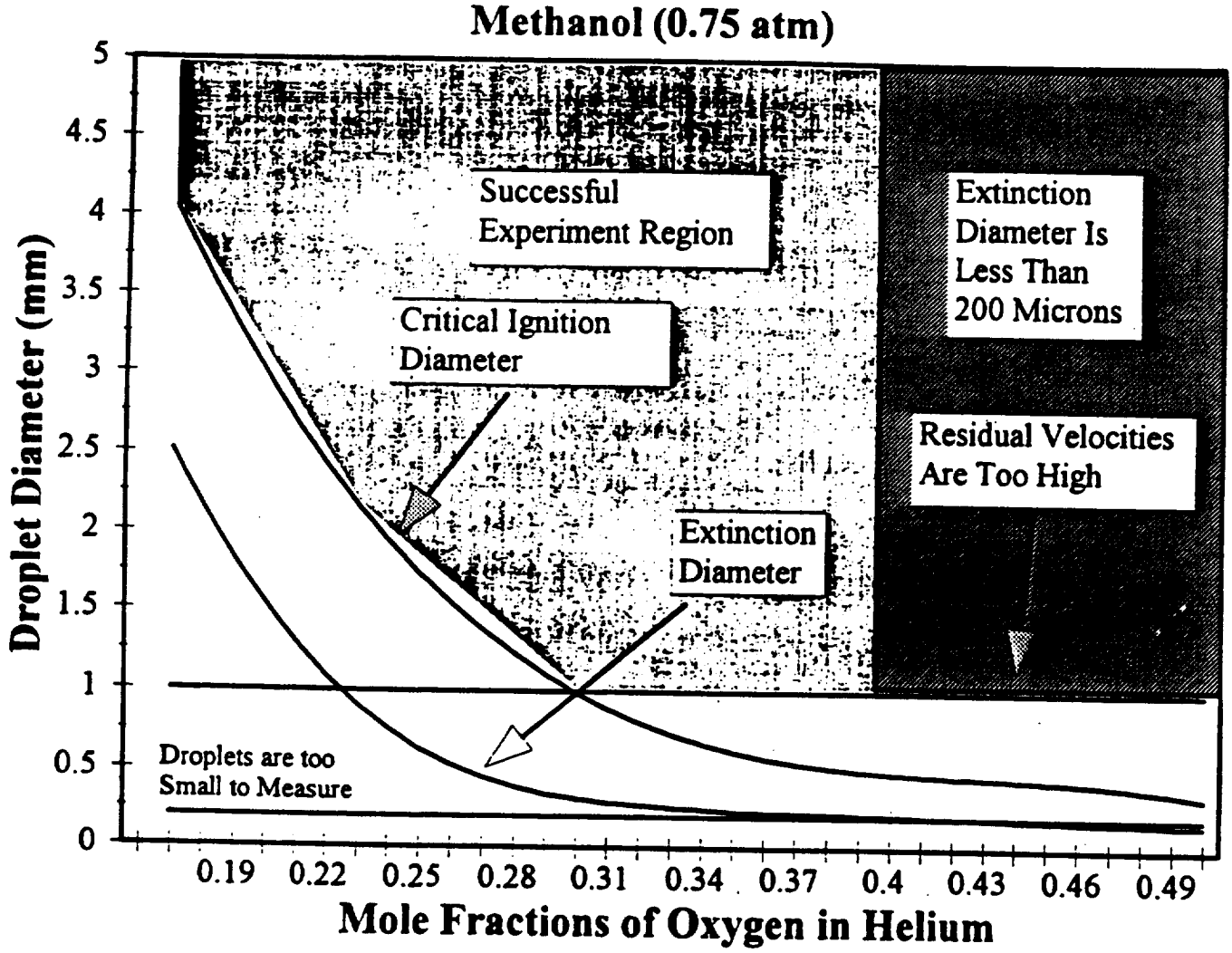

Figure 27. Experimental Test Matrix Envelope for Methanol Droplet Combustion in Helium-Oxygen Mixtures at 0.75 Atmospheres Pressure.

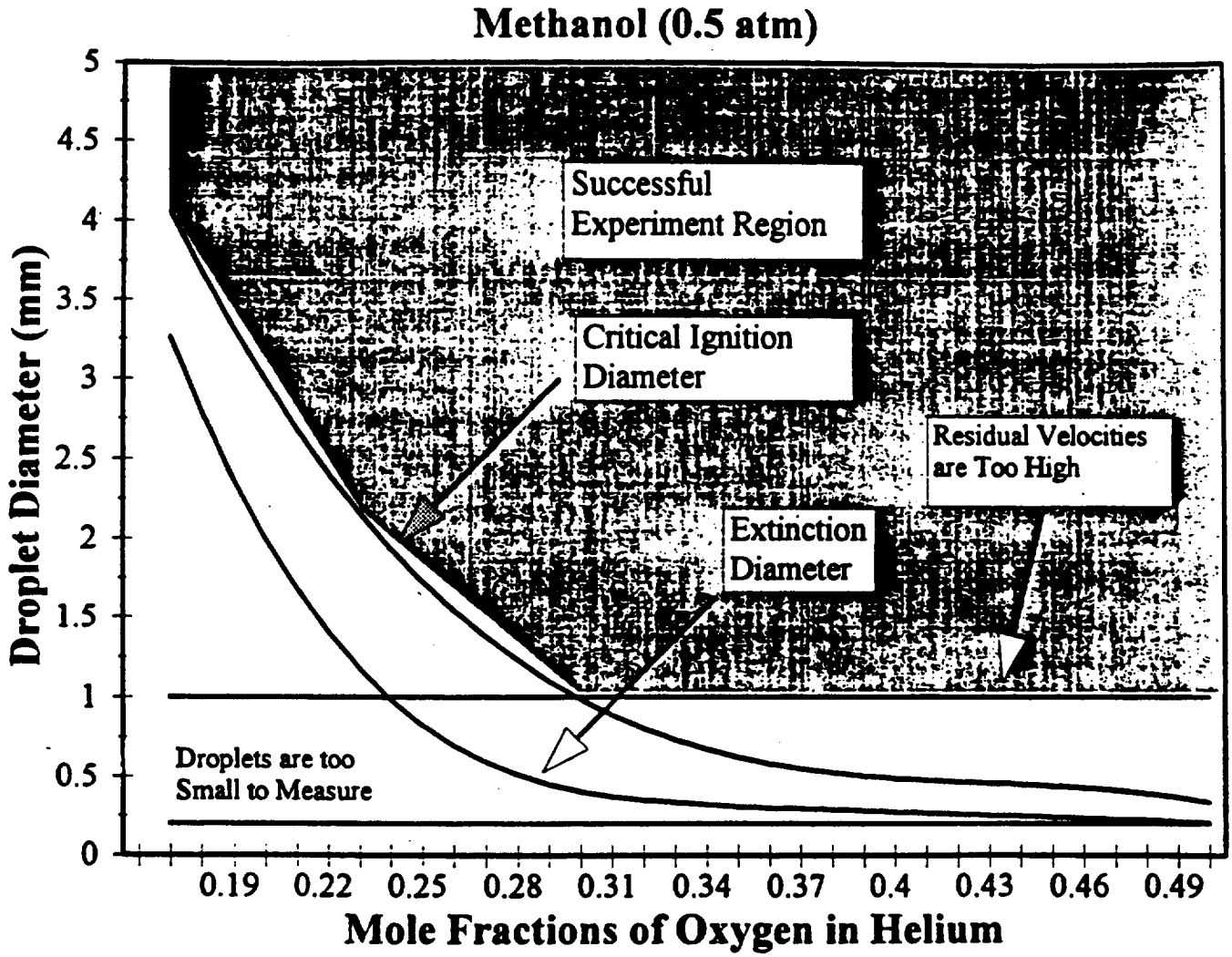

Figure 28. Experimental Test Matrix Envelope for Methanol Droplet Combustion in Helium-Oxygen Mixtures at 0.50 Atmospheres Pressure.

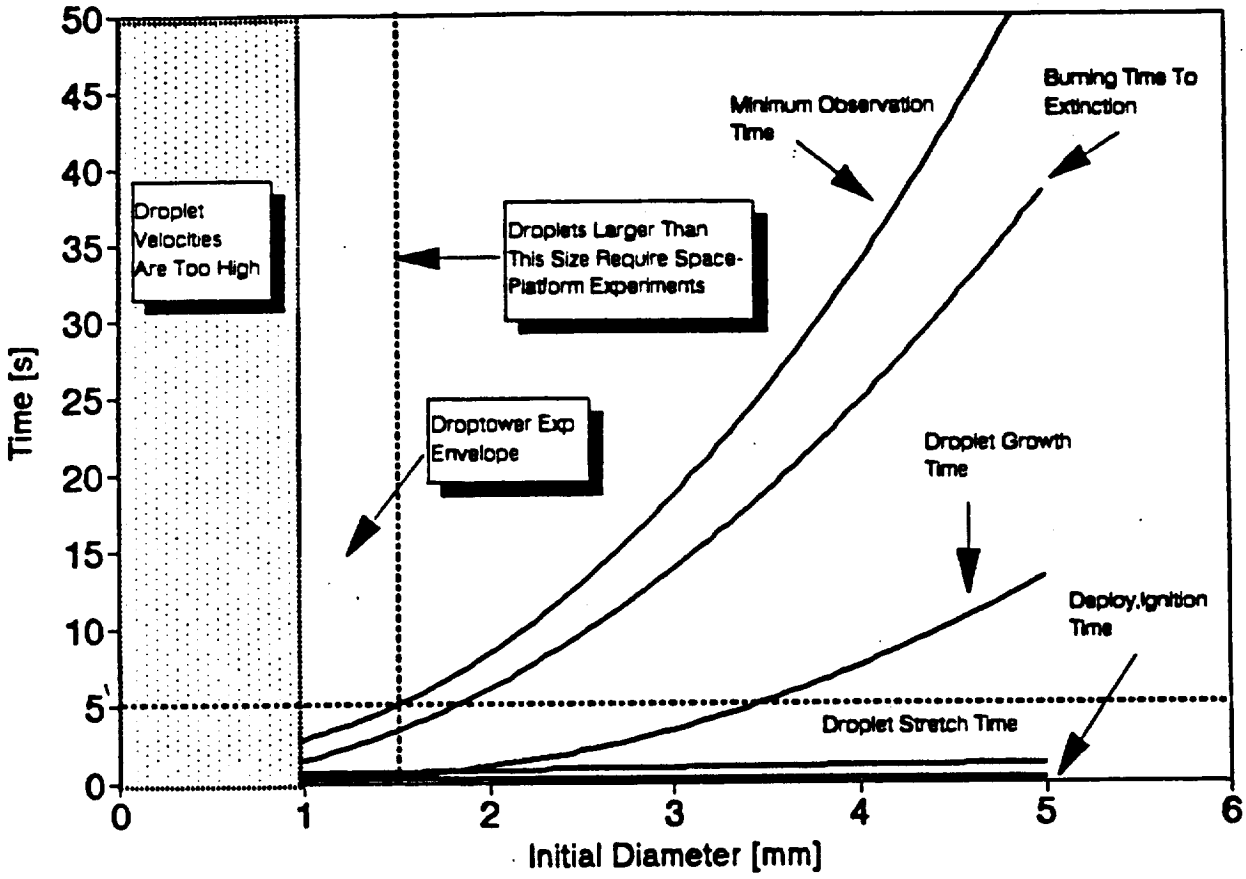

Figure 29. Experimental Test Time Requirements for the Combustion of N-Heptane Droplets in Helium-Oxygen Atmospheres at One Atmosphere Pressure.